

The reef-building coral *Siderastrea siderea* exhibits parabolic responses to ocean acidification and warming

Karl D. Castillo, Justin B. Ries, John F. Bruno and Isaac T. Westfield

Proc. R. Soc. B 2014 **281**, 20141856, published 5 November 2014

Supplementary data

["Data Supplement"](#)

<http://rsob.royalsocietypublishing.org/content/suppl/2014/11/05/rsob.2014.1856.DC1.html>

References

[This article cites 66 articles, 6 of which can be accessed free](#)

<http://rsob.royalsocietypublishing.org/content/281/1797/20141856.full.html#ref-list-1>

open access

This article is free to access

Subject collections

Articles on similar topics can be found in the following collections

[ecology](#) (1804 articles)

[environmental science](#) (300 articles)

[physiology](#) (152 articles)

Email alerting service

Receive free email alerts when new articles cite this article - sign up in the box at the top right-hand corner of the article or click [here](#)



Cite this article: Castillo KD, Ries JB, Bruno JF, Westfield IT. 2014 The reef-building coral *Siderastrea siderea* exhibits parabolic responses to ocean acidification and warming.

Proc. R. Soc. B **281**: 20141856.

<http://dx.doi.org/10.1098/rspb.2014.1856>

Received: 17 August 2014

Accepted: 1 October 2014

Subject Areas:

ecology, environmental science, physiology

Keywords:

tropical scleractinian coral, calcification, ocean warming, ocean acidification, *Siderastrea siderea*, Caribbean

Author for correspondence:

Karl D. Castillo

e-mail: karl_castillo@unc.edu

Electronic supplementary material is available at <http://dx.doi.org/10.1098/rspb.2014.1856> or via <http://rspb.royalsocietypublishing.org>.

The reef-building coral *Siderastrea siderea* exhibits parabolic responses to ocean acidification and warming

Karl D. Castillo¹, Justin B. Ries^{1,2}, John F. Bruno³ and Isaac T. Westfield^{1,2}

¹Department of Marine Sciences, University of North Carolina at Chapel Hill, Chapel Hill, NC 27599–3300, USA

²Department of Marine and Environmental Sciences, Marine Science Center, Northeastern University, Nahant, MA 01908, USA

³Department of Biology, University of North Carolina at Chapel Hill, Chapel Hill, NC 29599–3280, USA

Anthropogenic increases in atmospheric CO₂ over this century are predicted to cause global average surface ocean pH to decline by 0.1–0.3 pH units and sea surface temperature to increase by 1–4°C. We conducted controlled laboratory experiments to investigate the impacts of CO₂-induced ocean acidification ($p\text{CO}_2 = 324, 477, 604, 2553 \mu\text{atm}$) and warming (25, 28, 32°C) on the calcification rate of the zooxanthellate scleractinian coral *Siderastrea siderea*, a widespread, abundant and keystone reef-builder in the Caribbean Sea. We show that both acidification and warming cause a parabolic response in the calcification rate within this coral species. Moderate increases in $p\text{CO}_2$ and warming, relative to near-present-day values, enhanced coral calcification, with calcification rates declining under the highest $p\text{CO}_2$ and thermal conditions. Equivalent responses to acidification and warming were exhibited by colonies across reef zones and the parabolic nature of the corals' response to these stressors was evident across all three of the experiment's 30-day observational intervals. Furthermore, the warming projected by the Intergovernmental Panel on Climate Change for the end of the twenty-first century caused a fivefold decrease in the rate of coral calcification, while the acidification projected for the same interval had no statistically significant impact on the calcification rate—suggesting that ocean warming poses a more immediate threat than acidification for this important coral species.

1. Introduction

Atmospheric $p\text{CO}_2$ has increased from pre-industrial levels of *ca* 280 μatm to current levels exceeding 400 μatm [1,2], primarily due to the burning of fossil fuels, cement production and deforestation. This anthropogenic elevation of atmospheric $p\text{CO}_2$ has already decreased surface ocean pH by *ca* 0.1 pH unit [3]. Atmospheric $p\text{CO}_2$ is predicted to exceed 600 μatm by the end of the twenty-first century [4], which would cause surface ocean pH to decline by an additional 0.3 pH units [5,6]. This process of 'ocean acidification' reduces the carbonate ion concentration of seawater, which in turn reduces its saturation with respect to the calcium carbonate mineral aragonite, from which scleractinian corals and other marine invertebrates and algae build their protective shells and skeletons.

Atmospheric $p\text{CO}_2$ is also a greenhouse gas and its elevation has caused sea surface temperatures within the habitats of tropical scleractinian corals to increase by as much as 0.7°C over the past several decades [7,8]. The relationship between seawater temperature and calcification rates of tropical corals has been well explored [9–12]. In general, calcification rate increases with increasing seawater temperature up to an optimal temperature, which typically coincides with the mean summer seawater temperature of the coral's natural habitat [11]. At sufficiently elevated temperatures, corals lose their symbionts through a process known as bleaching, resulting in a further decline in calcification. Because maximum summertime temperatures on tropical reefs already approach the temperature at which corals bleach

[13], even a small increase in average seawater temperature may negatively impact their fitness.

The number of studies investigating the impacts of ocean acidification on coral calcification has increased exponentially [14–20], with several reviews published on the subject [21–23]. With each additional study, it is increasingly apparent that the calcification response of scleractinian corals to ocean acidification varies widely among taxa [16,20,24,25], and can vary within the same coral species when other experimental parameters (e.g. feeding, light, temperature, method of acidification) are modified [20,24]. Many of these experimental studies have shown that calcification rates of scleractinian corals decline relatively linearly with reductions in seawater pH [15,16,19,26–35]. However, other experimental studies have shown that scleractinian corals can also exhibit no response, a nonlinear threshold response or even a positive response to CO₂-induced reductions in seawater pH [14,18,36–39]. The complexities of the relationship between seawater pH and calcification rates of scleractinian corals are compounded by interactions between thermal and pH stress that are still not fully understood. For example, the negative effects of reduced seawater pH on coral calcification have been shown to increase under elevated temperatures, suggesting a synergistic effect [30,36,40], while other studies have shown that elevated temperature has either no effect or a mitigating effect on the response of scleractinian corals to ocean acidification [25,29,38,41,42]. This variability in corals' calcification response to ocean acidification, compounded by the interactive effects of other stressors, complicates efforts to predict and potentially mitigate the impacts of CO₂-induced ocean acidification on coral reefs.

Although the most adverse impacts on corals may arise from the combined effects of acidification and warming, the objective of this study was to isolate the impacts of these two stressors. Here, we present results of 95-day laboratory experiments designed to investigate the impacts of CO₂-induced ocean acidification (*p*CO₂ (s.d.); 324 (89), 477 (83), 604 (107) and 2553 (506) μ atm) and warming (temperature (s.d.); 25 (0.14), 28 (0.24) and 32 (0.17)°C) on calcification rates of the tropical reef-building zooxanthellate coral *Siderastrea siderea*—an important and ubiquitous component of Caribbean reef systems [43].

2. Material and methods

(a) Coral collection, transportation and maintenance

In July 2011, eighteen 20–30-year-old colonies of *S. siderea* were collected by hammer and chisel at 3–5 m depth from near shore, backreef and forereef reef zones in southern Belize [8] (see the electronic supplementary material for a detailed description of coral collection sites). Whole corals were transported to the Aquarium Research Center at the University of North Carolina at Chapel Hill by aeroplane. At UNC-Chapel Hill, each coral colony was sectioned into 18 comparatively sized specimens (surface area: 3 \times 2 cm; thickness: 1 cm) with a diamond-embedded petrographic saw and glued with cyanoacrylate to acrylic microscope slides. The coral specimens were allowed to recover for 30 days under laboratory conditions in two 500 l recirculating artificial seawater systems maintained at a salinity of 35, temperature of 28°C and an irradiance of *ca* 250 μ mol photons m⁻² s⁻¹. The corals were visually inspected each day of the recovery period and no evidence of bleaching or disease was observed. The corals were then acclimated for 15 days following the recovery period, after which the coral specimens were incrementally exposed to the modified *p*CO₂ and thermal conditions.

(b) Growth conditions

(i) Ocean acidification experiment

Siderastrea siderea coral specimens from each of the 18 colonies were reared for 95 days (5 August–8 November 2011) in each of twelve 38 l glass tanks (18 specimens per tank; 216 specimens in total) filled with artificial seawater formulated at a salinity (s.d.) of 35.13 (0.32) with *Instant Ocean Sea Salt* and deionized water. Although the trace elemental composition of *Instant Ocean Sea Salt* differs subtly from that of natural seawater, its major and minor elemental composition and its carbonate chemistry are the most similar to natural seawater when compared with eight other commercial sea salt mixes [44]. Four CO₂ partial pressures (s.d.) (324 (89), 477 (83), 604 (107), 2553 (506) μ atm), corresponding to a near-pre-industrial, a near-present-day, an end-of-century and an extreme year 2500 *p*CO₂ level were selected to define the shape of the *p*CO₂-calcification response curve for *S. siderea*. CO₂ partial pressures were established by mixing pure CO₂ with CO₂-free compressed air (CO₂ was removed with a Parker Hannifan FTIR Purge Gas Generator) using high-precision digital solenoid-valve-based mass flow controllers (Aalborg Instruments and Controls; Orangeburg, NY, USA). The experimental seawater was bubbled with microporous ceramic airstones into triplicate glass tanks (12 total). The *p*CO₂ of the mixed gases was measured with a Qubit S151 infrared *p*CO₂ analyser (Qubit Systems; Kingston, Ontario, Canada) calibrated with certified air-CO₂ gas standards (precision = \pm 2.0%; accuracy = \pm 1.8%). Coral specimens from the 18 colonies were reared in each of the 12 replicate tanks. The *p*CO₂ treatments were maintained at an average temperature (s.d.) of 28.10 (0.28)°C.

(ii) Temperature experiment

Experimental growth conditions for the temperature experiment were similar to those for the acidification experiment described above. *Siderastrea siderea* coral specimens from each of the 18 colonies were reared for 95 days (5 August–8 November 2011) in each of nine 38 l glass tanks (18 specimens per tank; 162 specimens in total) maintained at seawater temperatures (s.d.) of 25.01 (0.14), 28.16 (0.24), and 32.01 (0.17)°C. Salinity (s.d.) was maintained at 35.01 (0.12) by dissolving *Instant Ocean Sea Salt* in deionized water. These temperatures correspond to the corals' approximate annual minimum, mean and maximum seawater temperature as determined from more than 10 years (2002–2014) of *in situ* seawater temperature records obtained near the coral collection sites [8,45,46]. Thus, this range of temperatures was selected to capture this species' calcification response to the temperature variability occurring at present within a given year, as well as to the range of average annual seawater temperatures predicted for the next century. Coral specimens were reared in triplicate glass tanks at each of the three temperatures (nine tanks total). Mixed gas with an average *p*CO₂ (s.d.) of 488 (88) μ atm was bubbled with microporous ceramic airstones into the tanks. The *p*CO₂ of the temperature treatments were slightly higher than present-day atmospheric value of 400 μ atm due to slightly elevated *p*CO₂ in the aquarium culture laboratory. Nevertheless, the pH range in the temperature experiment (7.9–8.0) was within the range observed for present-day reefs [47].

(c) Tank conditions

Seawater within each tank was continuously filtered (757 l h⁻¹) with a power filter. Circulation and turbulence of seawater was enhanced with a 400 l h⁻¹ powerhead. Each tank was covered with a transparent 3-mm Plexiglas sheet and both the tank and filtration system were wrapped with cellophane to promote equilibration between the gas mixtures and the experimental seawaters and to minimize evaporative water loss. The tanks were illuminated for 12 h each day with compact fluorescent lights (ultra-actinic and white; 96 W, 10000 K) and with standard white fluorescent lights (32 W, T8

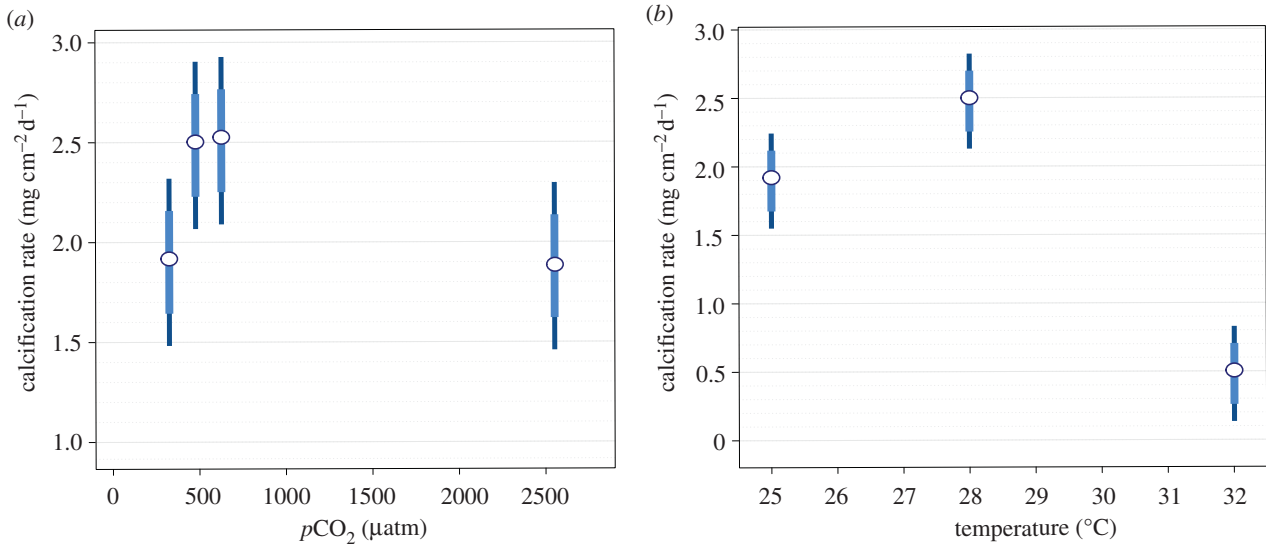


Figure 1. Parabolic calcification responses of the coral *S. siderea* to elevated $p\text{CO}_2$ and temperature across the 95-day experiments. (a) Calcification rates for corals at mean $p\text{CO}_2$ (s.d.) of 324 (89), 477 (83), 604 (107) and 2553 (506) μatm and at mean temperature (s.d.) of 28.10 (0.28) °C. (b) Calcification rates at mean temperatures (s.d.) of 25.01 (0.14), 28.16 (0.24) and 32.01 (0.17) °C and at mean $p\text{CO}_2$ (s.d.) of 488 (88) μatm . Ninety-five per cent (thin bars) and 83.5% (thick bars) confidence intervals of the means are shown.

6500 K), with a maximum photosynthetically active radiation (PAR) of ca 250 $\mu\text{mol photons m}^{-2} \text{s}^{-1}$. The intensity and timing of the prescribed irradiance within the tanks was designed to replicate the light cycle of the corals' native habitat (see the electronic supplementary material for a detailed description of light conditions). PAR in the field and in the experimental tanks was measured using a LI-1400 datalogger affixed with a LI-192 underwater quantum sensor (LI-COR; Lincoln, Nebraska; see the electronic supplementary material, figures S1 and S2).

The nominal 28 and 32 °C temperature treatments were maintained with 50-W heaters, while the 25 °C treatment was maintained with a 1-hp aquarium chiller paired with a 50-W heater for stability. Seventy-five per cent seawater changes were performed weekly. Seawater pH and temperature returned to target values within 60 min of water changes. Each week, 250 ml seawater samples were obtained in ground-glass-stoppered borosilicate glass bottles for analysis of dissolved inorganic carbon and total alkalinity (TA). Seawater samples were obtained midway between weekly water changes in order to acquire average values for the water chemistry parameters in the treatment tanks. Small aliquots of deionized water were periodically added to the experimental tanks in order to replenish water lost through evaporation, thereby maintaining target salinity (35). Each coral specimen was hand-fed 20 mg of frozen *Artemia* sp. every other day using a 1-ml transfer pipette. Feeding trials conducted prior to the start of the experiment revealed that this amount of food was sufficient to adequately nourish the coral specimens.

(d) Measurement and calculation of carbonate system parameters

Weekly seawater samples were analysed for DIC via coulometry (UIC 5400) and for TA via closed-cell potentiometric Gran titration calibrated with certified TA/DIC standards (see the electronic supplementary material for detailed methods). Temperature, salinity, and pH were determined via standard methods [48] approximately every other day. Additional carbonate system parameters (seawater $p\text{CO}_2$, pH, carbonate ion concentration, bicarbonate ion concentration, aqueous CO_2 , and aragonite saturation state) were calculated with the program CO₂SYS [49], using Roy *et al.* [50] values for K_1 and K_2 carbonic acid constants, the Mucci [51] value for the stoichiometric aragonite solubility product and an atmospheric pressure of 1.015 atm (see tables S1 and S2 and

figures S3 and S4 of the electronic supplementary material for seawater chemistry data).

(e) Quantification of calcification rates via buoyant weighing

Siderastrea siderea calcification rates were estimated using an empirically calibrated buoyant weight technique [14,52] (see the electronic supplementary material for empirical derivation of the buoyant weight–dry weight relationship for this species (figure S5)).

Calcification rates were estimated from the change in the coral specimen's dry weight normalized to its surface area and observational interval. Coral surface area was quantified from scaled top-view photographs of each coral specimen using the imaging software IMAGE J.

(f) Statistical analyses

Hierarchical mixed-effects models were employed to account for the combined repeated-measures/split-plot design to assess the overall effect of treatment on *S. siderea* calcification rates for the 95-day experiments and the impact of treatment duration on coral calcification response to warming and acidification (see the electronic supplementary material for details of statistical methods employed and tables S3 and S4 for description of observational intervals). All mixed models were estimated with the lme4 package [53] of R 3.0.2 [54].

Data are archived in the US National Science Foundation's Biological and Chemical Oceanography Database at (http://data.bco-dmo.org/jg/dir/test/OA_MarineCalcifiers/).

3. Results

(a) Ocean acidification experiment

Calcification rates for the coral *S. siderea* exhibited a parabolic response to increasing atmospheric $p\text{CO}_2$ (figure 1a). Over the entire 95-day experiment, calcification rates increased from the near-pre-industrial $p\text{CO}_2$ value of 324 μatm to the near-present-day value of 477 μatm , remained relatively unchanged at the predicted end-of-century value of 604 μatm and returned to near-pre-industrial rates at six-times the modern $p\text{CO}_2$ value of 2553 μatm (see the electronic supplementary material, table S5).

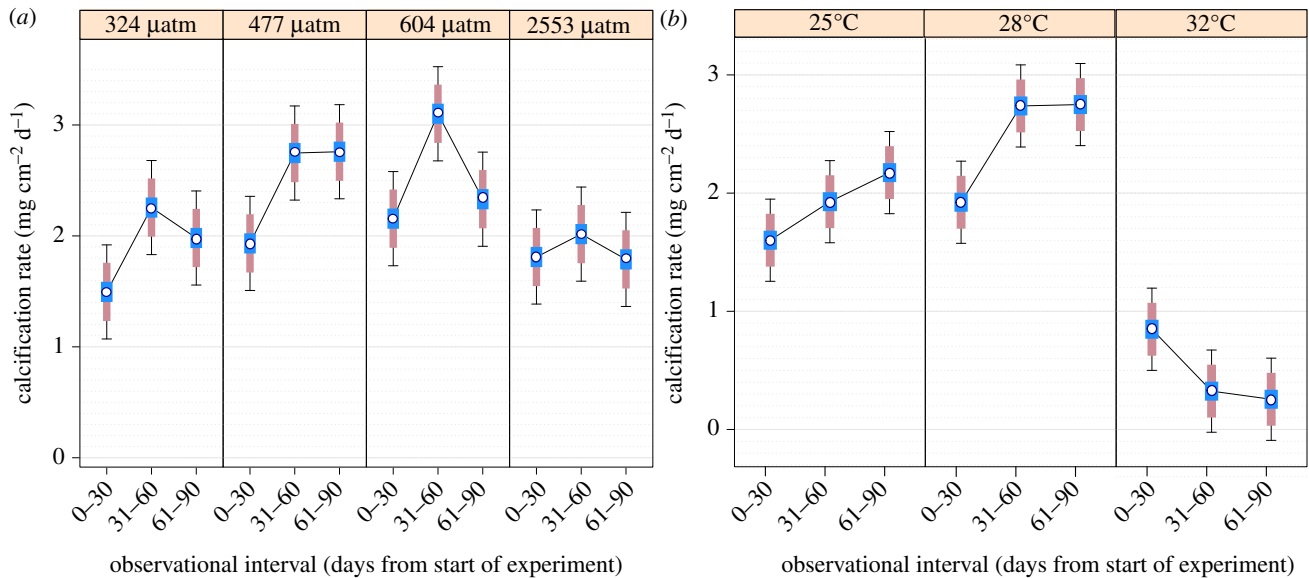


Figure 2. Effects of exposure duration on *S. siderea* coral calcification response to $p\text{CO}_2$ and temperature. (a) Calcification rates at three monthly observational intervals for *S. siderea* corals reared at mean $p\text{CO}_2$ (s.d.) of 324 (89), 477 (83), 604 (107) and 2553 (506) μatm and maintained at mean temperature (s.d.) of 28.10 (0.28)°C. (b) Calcification rates at three monthly observational intervals for *S. siderea* corals reared at temperatures (s.d.) of 25.01 (0.14), 28.16 (0.24) and 32.01 (0.17)°C and at mean $p\text{CO}_2$ (s.d.) of 488 (88). Ninety-five per cent confidence intervals (black bars) show precision of estimated calcification rates. Eighty-three and one-half per cent confidence intervals (pink bars) are for across-panel (i.e. across treatment) comparison. Forty-two and one-half per cent confidence intervals (blue bars) are for within-panel (i.e. within treatment) comparison.

(b) Temperature experiments

A parabolic calcification response pattern was also exhibited by the coral *S. siderea* in response to increasing seawater temperature (figure 1b). Over the entire 95-day experiment, calcification rates increased from the lower end of the corals' temperature range of 25°C to their average annual temperature of 28°C and then declined under a temperature of 32°C, near the upper end of their annual thermal range (see the electronic supplementary material, table S6).

(c) Effect of exposure duration on coral calcification response to CO₂-induced acidification and warming

Differences in coral calcification rates were also assessed across three *ca* 30-day observational intervals (0–30, 31–60 and 61–90 days) using difference-adjusted confidence intervals [55,56] to assess the impact of duration of exposure to $p\text{CO}_2$ (see figure 2a and electronic supplementary material, table S7) and temperature treatments (see figure 2b and electronic supplementary material, table S8) on *S. siderea* calcification rates.

(i) Ocean acidification experiment

Comparisons *within* $p\text{CO}_2$ treatments (i.e. within-panel comparisons; figure 2a; confidence interval = blue bars) reveal that calcification rates for *S. siderea* corals reared at 324, 477, 604 and 2553 μatm increased significantly between the first observational interval (0–30 days) and the second observational interval (31–60 days), but declined (except for corals reared at 477 μatm , which remained constant) between the second observational interval and the third observation interval (61–90 days). Notably, calcification rates for the third observational interval were significantly greater than at the first observational interval for the two lowest $p\text{CO}_2$ treatments, but not for the two highest $p\text{CO}_2$ treatments.

Comparisons *between* $p\text{CO}_2$ treatments (i.e. across-panel comparisons; figure 2a; confidence interval = pink bars)

reveal that calcification response patterns to acidification are parabolic for each of the three observational intervals.

(ii) Temperature experiment

Comparisons *within* temperature treatments (i.e. within-panel comparisons; figure 2b; confidence interval = blue bars) reveal that calcification rates increased across the three observational intervals for corals reared at 25°C, increased across the first two observational intervals for corals reared at 28°C and decreased across the first two observational intervals for corals reared at 32°C. However, coral calcification rates were constant between the second and third observational intervals for corals reared at 28 and 32°C.

Comparisons *between* temperature treatments (i.e. across-panel comparisons; figure 2b; confidence interval = pink bars) reveal that calcification response patterns to warming are parabolic for each of the three observational intervals.

(d) Effect of reef zone on coral calcification response to CO₂-induced acidification and warming

Calcification rates of *S. siderea* corals were not significantly different across reef zones (i.e. forereef versus backreef versus near shore colonies) within any of the $p\text{CO}_2$ or temperature treatments (see the electronic supplementary material, figures S7 and S8, and tables S9 and S10).

4. Discussion

(a) Parabolic calcification response to acidification

Calcification rates within the coral *S. siderea* increased with moderate elevations in $p\text{CO}_2$, but declined with extreme elevation, yielding a parabolic response to CO₂-induced ocean acidification. Previous experimental studies, most of which did not use a pre-industrial $p\text{CO}_2$ level, showed that corals

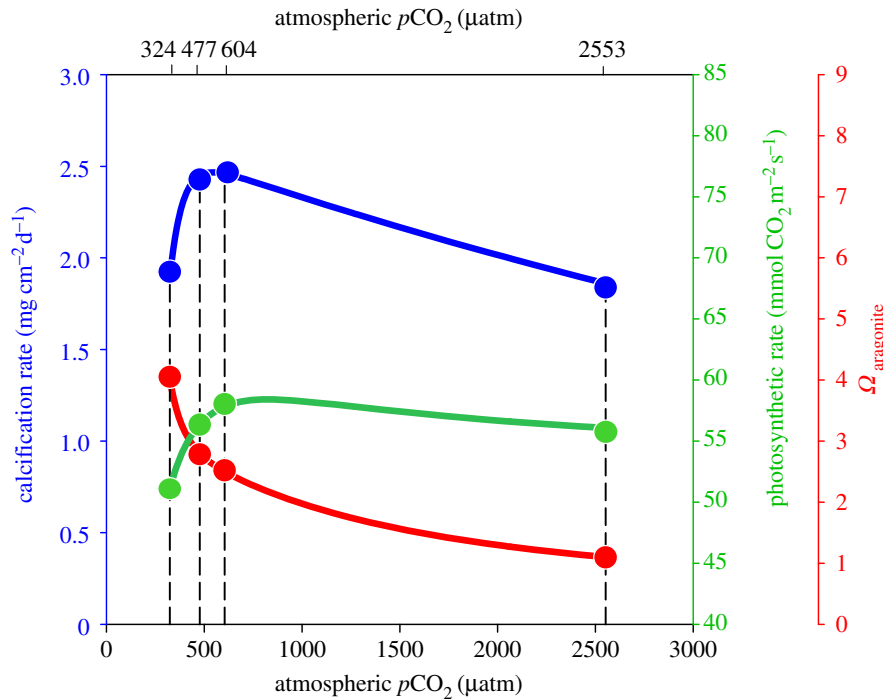


Figure 3. Conceptual diagram (constrained by study results) illustrating how photosynthesis (green curve; estimated from measured F_v/F_m using empirical $F_v/F_m - \text{ETR}_{\text{max}}$ relationship from Frade *et al.* [58] (see the electronic supplementary material, figure S6)) and aragonite saturation state (Ω_{A}) (red curve; data from this study) interact to generate the corals' parabolic calcification response (blue curve; data from this study) to rising atmospheric $p\text{CO}_2$.

exhibit either no response [16,25,30,40], a threshold-negative response [14] or a linear negative response to CO_2 -induced ocean acidification [15,16,20,25,30], although in a recent study the cold-water coral *Lophelia pertusa* exhibited slightly enhanced calcification under acidified conditions [57].

There are two important factors involved in the process of coral calcification that are impacted by CO_2 -induced ocean acidification in potentially opposite ways: seawater saturation state with respect to the calcium carbonate mineral aragonite (Ω_{A}) and photosynthesis (figure 3). Increasing $p\text{CO}_2$ causes seawater pH to decline, which results in a reduction in carbonate ion concentration ($[\text{CO}_3^{2-}]$) and thus Ω_{A} , which should impair calcification (red curve, figure 3). Conversely, increasing $p\text{CO}_2$ causes the amount of CO_2 dissolved in seawater, i.e. aqueous CO_2 ($\text{CO}_2\text{-aq}$), to increase, which should fertilize photosynthesis by the coral's algal symbionts, yielding more photosynthate and thus more energy for coral calcification [39] (green curve, figure 3). Recent studies on *Symbiodinium* phylotypes previously isolated from reef-building corals suggest that the diffusive uptake of $\text{CO}_2\text{-aq}$ from the external medium within at least one of four *Symbiodinium* phylotypes is at least partially dependent upon the concentration of $\text{CO}_2\text{-aq}$ [59,60]. Thus, CO_2 -induced ocean acidification may increase the concentration of $\text{CO}_2\text{-aq}$ available to this symbiont type, potentially elevating photosynthetic capacity of the coral holobiont that could confer supplemental energy for calcification.

A generalized model of the relationship between aragonite saturation state (red curve), rate of photosynthesis (green curve) and rate of coral calcification (blue curve)—each constrained by measurements from the present experiment (solid circles)—is rendered in figure 3. Aragonite saturation states and rates of calcification were measured directly, while rates of photosynthesis were estimated indirectly from pulse amplitude modulated fluorometry (see the electronic supplementary material (figure S6) for details of how photosynthetic rates

were estimated). This analysis reveals that rates of symbiont photosynthesis (green curve in figure 3) increase with increasing $p\text{CO}_2$ from 324 to 604 μatm , and then decline slightly between 604 and 2553 μatm . Thus, moderate elevations in $p\text{CO}_2$ (324–604 μatm) appear to enhance photosynthesis of *Symbiodinium* within *S. siderea*, while extreme elevations cause symbiont photosynthesis to plateau or slightly decline [59], perhaps because CO_2 is no longer limiting for photosynthesis at these elevated levels. The model (figure 3) suggests that calcification rates for *S. siderea* corals may increase (figure 1a) as $p\text{CO}_2$ rises from 324 to 477 μatm because the challenge of calcifying under lower Ω_{A} is outweighed by the benefits of enhanced symbiont photosynthesis (e.g. increased energy and/or more favourable carbonate chemistry at the site of calcification) under moderately elevated $p\text{CO}_2$ (324–477 μatm ; figure 3). As $p\text{CO}_2$ rises from 477 to 604 μatm , Ω_{A} continues to decrease while the benefits to calcification conferred by CO_2 -enhanced photosynthesis should continue to increase. It is therefore possible that the observed lack of change in coral calcification rate from 477 to 604 μatm (figure 1a) results from the benefit of enhanced photosynthesis being effectively neutralized, in terms of its impact on coral calcification rate, by the decline of Ω_{A} towards undersaturated conditions. Likewise, the increase in $p\text{CO}_2$ from 604 μatm to the ultra-high value of 2553 μatm translates to an extreme decrease in Ω_{A} —nearly to the point of undersaturation ($\Omega_{\text{A}} < 1$)—which may outweigh the now relatively minor benefit of CO_2 -enhanced photosynthesis as the corals' symbionts transition away from strict CO_2 -limitation [30,61] (figure 3), resulting in the substantial decline in coral calcification rate observed across the 604–2553 μatm range (figure 1a).

The surprising ability of *S. siderea* corals to continue building new skeletal material under all experimental treatments, even at the nearly undersaturated ($\Omega_{\text{A}} < 1$) level of 2553 μatm , may arise from the corals' capacity to manipulate the carbonate chemistry at their site of calcification [14,31,62–64].

Some calcifying organisms, by elevating pH of their calcifying fluid, facilitate the deprotonation of bicarbonate ions—whose concentrations are increased under conditions of elevated $p\text{CO}_2$ —resulting in elevated carbonate ion concentrations and Ω_{A} at the site of calcification. Indeed, *in situ* microelectrode measurements of pH within the calcifying medium of the tropical scleractinian coral *Galaxea fascicularis* reveal greater than one pH unit increase above that of ambient seawater [65]. Similar increases in pH have been measured within the calcifying fluid of the temperate scleractinian coral *Astrangia poculata* [15] and inferred for the tropical scleractinian corals *Stylophora pistillata* [66], *Porites* sp. [31], *Cladocora caespitosa* [67], *Desmophyllum dianthus* [68], *Favia fragum* [69] and various species of cold-water scleractinia [70]. A recent study also reveals spatial variations in the calcifying fluid pH of the coral *S. pistillata*, with polyp tissue exhibiting apparently greater control over calcifying fluid pH than coenosarc tissue [71].

Yet, despite the ability of *S. siderea* corals to continue building new skeletal material at $p\text{CO}_2$ of 2553 μatm , the decline in calcification rate from 604 to 2553 μatm reveals there is a limit to the extent that they can manipulate carbonate chemistry at their site of calcification under conditions of elevated $p\text{CO}_2$ —beyond which coral calcification rates will decline.

(b) Parabolic calcification response to warming

A parabolic response pattern was also exhibited by the *S. siderea* corals in response to increasing seawater temperature, with calcification increasing from 25 to 28°C, reaching a maximum at 28°C, and then decreasing from 28 to 32°C (figure 1b). This is consistent with a typical thermal performance curve, in which biological performance increases with rising temperature, reaches a maximum at an optimal temperature, and then declines as temperature continue to rise [72–74].

The parabolic shape of the thermal performance curve is usually attributed to a combination of thermodynamic effects of temperature on reaction rates and the destabilizing effects of temperature on a range of intermolecular interactions [75]. Specifically, the increase in coral calcification from 25 to 28°C may result from thermal acceleration of coral metabolism, including acceleration of zooxanthellate photosynthesis or increased rates of respiration by the coral animal, which would increase thermal energy (as described by the Arrhenius equation) and thus increase rates of chemical reactions involved in calcification [76]. The thermally driven increase in aragonite saturation state may also contribute to the increase in calcification rate observed between 25°C and 28°C. The waning phase of the thermal performance curve results from the destabilizing effects of temperature on a range of intermolecular interactions, ultimately leading to the destruction of the coral–dinoflagellate symbiosis—a process known as coral bleaching [13,77].

The parabolic shape of *S. siderea*'s calcification response to both warming and acidification suggests that parabolic responses to environmental stressors may be the norm and that linear responses arise when the range of the independent stress variable (e.g. temperature, $p\text{CO}_2$) is too narrow to capture the full parabolic geometry of the response pattern. However, our observation that the calcification responses of *S. siderea* to both warming and acidification are parabolic does not necessarily mean that the corals' response to future combined warming and acidification will be parabolic.

Although target temperature and $p\text{CO}_2$ levels were generally maintained throughout the 95-day experimental interval,

there was moderate variability in TA and associated carbonate system parameters within both sets of experiments. These variations in TA were driven by progressive sequestration of carbonate ions through the coral calcification process. Although weekly water changes were performed, only 75% of the experimental seawater was exchanged in order to avoid shocking the corals. Thus, 25% of the TA drawdown was passed on to the next week's treatment, causing the weekly drawdown in TA to be semi-cumulative throughout the duration of the experiment. This resulted in two trends in TA among treatments: variability in weekly TA within treatments and variability in average TA among treatments (see the electronic supplementary material, tables S1 and S2, and figures S3 and S4).

These trends were most pronounced in the temperature experiment due to the relatively large difference in average calcification rates between the 32°C (TA = 2725 μM) and 28°C (TA = 1951 μM) treatments, which translated to proportional differences in TA (and associated carbonate system parameters) between the treatments. However, after controlling for the effect of temperature on pH, the elevated TA in the 32°C only imparts an approximately 0.1 unit effect on pH relative to pH of the 28°C treatment. Differences in calcification rates between the high-calcification-rate $p\text{CO}_2$ treatments (i.e. 477, 604 μatm) and the low-calcification-rate $p\text{CO}_2$ treatments (i.e. 324, 2553 μatm) yielded similar but more muted trends in TA for the $p\text{CO}_2$ experiment.

Since elevated calcification was causing the decline in TA in both the temperature and $p\text{CO}_2$ experiments (rather than depressed TA causing the decline in calcification), corals exhibiting the slowest calcification rates occupied treatments with the highest, most geochemically favourable TA. Therefore, it is reasonable to conclude that the observed differences in TA among treatments only dampened the fundamental calcification trends that were observed, rather than modifying their directions. Had the intermediate $p\text{CO}_2$ and temperature treatments that supported the faster calcifying corals been fixed at the higher TAs that were maintained for the low and high $p\text{CO}_2$ and temperature treatments, then the faster calcifying corals in the intermediate treatments would have experienced higher aragonite saturation states and thus presumably exhibited even higher calcification rates—thereby enhancing the parabolic shape of the calcification trends observed in both experiments.

Many studies on coral calcification [78,79] use such coral-induced drawdown of TA in a closed system to estimate coral calcification rates (2 moles of TA = 1 mole of CaCO_3 produced), an approach known as the 'alkalinity anomaly technique'. Indeed, this approach is recommended as one of the 'best practices' for quantifying calcification rates in ocean acidification research [80]. Nevertheless, the observed differences in coral-induced drawdown of TA and associated carbonate system parameters among treatments should be duly considered in the interpretation of these results.

(c) Duration of exposure to CO_2 -induced acidification impacts coral calcification rate

The increase in calcification rates of *S. siderea* between the 0–30-day and the 31–60-day observational intervals suggests that the corals continued acclimating to their treatment conditions throughout these intervals (figure 2a), despite the prescribed acclimation period and gradual adjustment of temperature and $p\text{CO}_2$ to the treatment levels. The difference

in coral calcification rate between these two observational intervals suggests that a coral's response to an ocean acidification experiment is impacted by its duration of exposure, and may partly explain the wide range of calcification response patterns exhibited by identical or similar organisms in experiments that differ in their duration [14,16,22,23]. Despite these within-treatment differences in calcification rate across the three observational intervals, the corals exhibited comparably parabolic response patterns to acidification within each of the three observational intervals.

Although corals reared at 477 μatm maintained constant calcification after the second observational interval, calcification rates for corals reared at 324, 604 and 2553 μatm declined between the second and third observational intervals. Perhaps during shorter term exposure of these corals to elevated (604, 2553 μatm) or reduced (324 μatm) $p\text{CO}_2$, the corals are able to maintain their calcifying medium at a suitable Ω_{A} via pH regulation of the calcifying medium [66], which requires energy. More prolonged exposure to $p\text{CO}_2$ perturbation, however, may deplete the corals' lipid energy reserves, which would limit their ability to regulate Ω_{A} at the site of calcification, resulting in the reduced calcification rates evident in the third observational interval (61–90 days). *Siderastrea siderea* corals reared at the near-present-day $p\text{CO}_2$ level of 477 μatm would have experienced the least change in energetic demands associated with regulating carbonate chemistry at their site of calcification, which is consistent with their calcification rates remaining constant between the second and third observational intervals. Although it is assumed that calcification consumes more energy under acidified conditions [23,37], a recent study [25] shows that lipid reserves of four coral species did not decline after approximately 30 days as $p\text{CO}_2$ was elevated from 382 to 741 μatm . Thus, the findings of that study are not consistent with our assertion that *S. siderea* lipid reserves are progressively depleted when the corals are exposed to prolonged periods of acidification. These disparities may arise from interspecific differences in energetic demands of calcification or from differences in the duration of the corals' exposure to elevated $p\text{CO}_2$.

(d) Duration of exposure to warming impacts coral calcification rate

The increase in calcification rates across the three observational intervals for corals reared at 25°C suggests that they continued to acclimate to the low temperature conditions throughout the duration of the experiment. Conversely, the relative stabilization in calcification rates between the second and third observational intervals for corals reared at 28 and 32°C suggests that they had fully acclimated by the end of the second interval (figure 2b). Yet, despite these within-treatment differences in calcification rate across observational intervals, the corals' general calcification response patterns to warming were parabolic within each of the three observational intervals.

It is unlikely that the effects of exposure duration on the calcification response of *S. siderea* corals in this study simply arose

from the corals' experimental conditions differing from their natural habitat as such effects should have been constant among treatments and thus impacted corals in all treatments in approximately the same manner. This was not borne out in the experiments, as exposure duration generally had less of an impact on corals in the control treatments than on corals in the high/low $p\text{CO}_2$ and temperature treatments—suggesting that the variable effects of exposure duration were indeed linked to the experiments' independent variables (temperature and $p\text{CO}_2$).

(e) Near shore, backreef and forereef colonies exhibit equivalent responses to ocean acidification and warming

No statistically significant differences in calcification rates were observed among forereef, backreef and near shore colonies reared under replicate treatments in this study (see the electronic supplementary material, figures S7 and S8, and tables S9 and S10). However, it is possible that a longer experiment, across narrower ranges and finer increments of temperature, would reveal the differential responses among *S. siderea* corals from different reef zones that were evident in recently obtained cores of this species [8].

(f) Ocean warming poses a more immediate threat than ocean acidification for the coral *Siderastrea siderea*

This experimental study shows that calcification rates of *S. siderea* corals exposed to IPCC projected end-of-century tropical seawater temperatures (32°C) declined nearly 80% relative to the control treatment (28°C), while calcification rates for corals reared at IPCC projected end-of-century $p\text{CO}_2$ levels (604 μatm) were unchanged relative to the control treatment (477 μatm). Thus, given IPCC's projections for end-of-century climate and oceanic change [81], the results of this study suggest that ocean warming poses a more immediate threat than ocean acidification for the coral *S. siderea*. That said, interpretation of these isolated impacts of warming and acidification on coral calcification should be tempered by the understanding that these two stressors are occurring and will continue to occur in tandem.

Ethics statement. We thank the Belize Fisheries Department for providing permits for collecting and exporting coral samples.

Data accessibility. Data are archived in the US National Science Foundation's Biological and Chemical Oceanography Database at (http://data.bco-dmo.org/jg/dir/test/OA_MarineCalcifiers/).

Acknowledgements. J. Weiss is acknowledged for providing guidance on the statistical analyses. We thank B. Elder, E. Chow, K. Patel, R. Yost and D. Shroff for helping to maintain the experimental tanks.

Funding statement. This research was supported by the Carolina Postdoctoral Fellowship for Faculty Diversity (to K.D.C.), Seeding Postdoctoral Innovators in Research and Education (SPIRE; to K.D.C.), NOAA award nos. NA11OAR431016 and NA13OAR4310186 (to J.B.R. and K.D.C.) and NSF award nos. 1031995 and 1357665 (to J.B.R.). This is publication number 381 from the Northeastern University Marine Science Center.

References

- Keeling R, Piper S, Bollenbacher A, Walker J. 2009 Atmospheric CO_2 records from sites in the SIO air sampling network. In *Trends: a compendium of data on Global Change, Carbon Dioxide Information Analysis Center*. Oak Ridge, TN: Oak Ridge National Laboratory, US Department of Energy.
- Rahmstorf S, Cazenave A, Church JA, Hansen JE, Keeling RF, Parker DE, Somerville RJ. 2007 Recent climate observations compared to

- projections. *Science* **316**, 709. (doi:10.1126/science.1136843)
3. Raven J, Caldeira K, Elderfield H, Hoegh-Guldberg O, Liss P, Riebesell U, Shephard J, Turley C, Watson A. 2005 Ocean acidification due to increasing atmospheric carbon dioxide. Policy Document 12/05. London, UK: The Royal Society.
 4. Trenberth KE *et al.* 2007 In *Climate Change 2007: The Physical Science Basis Contribution of Working Group I to the Fourth Assessment Report of the Intergovernmental Panel on Climate Change* (eds S Solomon, D Qin, M Manning, Z Chen, M Marquis, KB Averyt, M Tignor, HL Miller). Cambridge, UK and New York, NY, USA: Cambridge University Press.
 5. Caldeira K, Wickett ME. 2003 Oceanography: anthropogenic carbon and ocean pH. *Nature* **425**, 365. (doi:10.1038/425365a)
 6. Orr JC *et al.* 2005 Anthropogenic ocean acidification over the twenty-first century and its impact on calcifying organisms. *Nature* **437**, 681–686. (doi:10.1038/nature04095)
 7. Kleypas JA, Danabasoglu G, Lough JM. 2008 Potential role of the ocean thermostat in determining regional differences in coral reef bleaching events. *Geophys. Res. Lett.* **35**, L03613. (doi:10.1029/2007GL032257)
 8. Castillo KD, Ries JB, Weiss JM, Lima FP. 2012 Decline of forereef corals in response to recent warming linked to history of thermal exposure. *Nat. Clim. Change* **2**, 756–760. (doi:10.1038/nclimate1577)
 9. Lough JM, Barnes DJ. 2000 Environmental controls on growth of the massive coral *Porites*. *J. Exp. Mar. Biol. Ecol.* **245**, 225–243. (doi:10.1016/S0022-0981(99)00168-9)
 10. De'ath G, Lough JM, Fabricius KE. 2009 Declining coral calcification on the Great Barrier Reef. *Science* **323**, 116–119. (doi:10.1126/science.1165283)
 11. Jokiel PL, Coles SL. 1977 Effects of temperature on the mortality and growth of Hawaiian reef corals. *Mar. Biol.* **43**, 201–208. (doi:10.1007/BF00402312)
 12. Cooper TF, De'ath G, Fabricius KE, Lough JM. 2008 Declining coral calcification in massive *Porites* in two nearshore regions of the northern Great Barrier Reef. *Glob. Change Biol.* **14**, 529–538. (doi:10.1111/j.1365-2486.2007.01520.x)
 13. Brown BE. 1997 Coral bleaching: causes and consequences. *Coral Reefs* **16**, S129–S138. (doi:10.1007/s003380050249)
 14. Ries J, Cohen A, McCorkle D. 2010 A nonlinear calcification response to CO₂-induced ocean acidification by the coral *Oculina arbuscula*. *Coral Reefs* **29**, 661–674. (doi:10.1007/s00338-010-0632-3)
 15. Holcomb M, Cohen A, McCorkle D. 2012 An investigation of the calcification response of the scleractinian coral *Astrangia poculata* to elevated pCO₂ and the effects of nutrients, zooxanthellae and gender. *Biogeosciences* **9**, 29–39. (doi:10.5194/bg-9-29-2012)
 16. Comeau S, Edmunds P, Spindel N, Carpenter R. 2013 The response of eight coral reef calcifiers to increasing partial pressure of CO₂ do not exhibit a tipping point. *Limnol. Oceanogr.* **58**, 388–398. (doi:10.4319/lo.2013.58.1.0388)
 17. Bramanti L *et al.* 2013 Detrimental effects of ocean acidification on the economically important Mediterranean red coral (*Corallium rubrum*). *Glob. Change Biol.* **19**, 1897–1908. (doi:10.1111/gcb.12171)
 18. Jury CP, Whitehead RF, Szmant AM. 2010 Effects of variations in carbonate chemistry on the calcification rates of *Madracis auretenra* (= *Madracis mirabilis* sensu Wells, 1973): bicarbonate concentrations best predict calcification rates. *Glob. Change Biol.* **16**, 1632–1644. (doi:10.1111/j.1365-2486.2009.02057.x)
 19. Edmunds PJ, Brown D, Moriarty V. 2012 Interactive effects of ocean acidification and temperature on two scleractinian corals from Moorea, French Polynesia. *Glob. Change Biol.* **18**, 2173–2183. (doi:10.1111/j.1365-2486.2012.02695.x)
 20. Anthony KRN, Kleypas AJ, Gattuso J-P. 2011 Coral reefs modify their seawater carbon chemistry—implications for impacts of ocean acidification. *Glob. Change Biol.* **17**, 3655–3666. (doi:10.1111/j.1365-2486.2011.02510.x)
 21. Hoegh-Guldberg O *et al.* 2007 Coral reefs under rapid climate change and ocean acidification. *Science* **318**, 1737–1742. (doi:10.1126/science.1152509)
 22. Doney SC, Fabry VJ, Feely RA, Kleypas JA. 2009 Ocean acidification: the other CO₂ problem. *Annu. Rev. Mar. Sci.* **1**, 169–192. (doi:10.1146/annurev.marine.010908.163834)
 23. Erez J, Reynaud S, Silverman J, Schneider K, Allemand D. 2011 Coral calcification under ocean acidification and global change. In *Coral reefs: an ecosystem in transition* (eds Z Dubinsky, N Stambler), pp. 151–176. Berlin, Germany: Springer.
 24. Chan NCS, Connolly SR. 2013 Sensitivity of coral calcification to ocean acidification: a meta-analysis. *Glob. Change Biol.* **19**, 282–290. (doi:10.1111/gcb.12011)
 25. Schoepf V *et al.* 2013 Coral energy reserves and calcification in a high-CO₂ world at two temperatures. *PLoS ONE* **8**, e75049. (doi:10.1371/journal.pone.0075049)
 26. Marubini F, Atkinson MJ. 1999 Effects of lowered pH and elevated nitrate on coral calcification. *Mar. Ecol. Prog. Ser.* **188**, 117–121. (doi:10.3354/meps188117)
 27. Langdon C, Takahashi T, Sweeney C, Chipman D, Goddard J, Marubini F, Aceves H, Barnett H, Atkinson MJ. 2000 Effect of calcium carbonate saturation state on the calcification rate of an experimental coral reef. *Glob. Biogeochem. Cycles* **14**, 639–654. (doi:10.1029/1999gb001195)
 28. Leclercq NIC, Gattuso JEANP, Jaubert JEAN. 2000 CO₂ partial pressure controls the calcification rate of a coral community. *Glob. Change Biol.* **6**, 329–334. (doi:10.1046/j.1365-2486.2000.00315.x)
 29. Langdon C, Atkinson MJ. 2005 Effect of elevated pCO₂ on photosynthesis and calcification of corals and interactions with seasonal change in temperature/irradiance and nutrient enrichment. *J. Geophys. Res.* **110**, C09S07. (doi:10.1029/2004jc002576)
 30. Anthony KRN, Kline DI, Diaz-Pulido G, Dove S, Hoegh-Guldberg O. 2008 Ocean acidification causes bleaching and productivity loss in coral reef builders. *Proc. Natl Acad. Sci. USA* **105**, 17 442–17 446. (doi:10.1073/pnas.0804478105)
 31. Krief S, Hendy EJ, Fine M, Yam R, Meibom A, Foster GL, Shemesh A. 2010 Physiological and isotopic responses of scleractinian corals to ocean acidification. *Geochim. Cosmochim. Acta* **74**, 4988–5001. (doi:10.1016/j.gca.2010.05.023)
 32. Marubini F, Ferrier-Pagès C, Furla P, Allemand D. 2008 Coral calcification responds to seawater acidification: a working hypothesis towards a physiological mechanism. *Coral Reefs* **27**, 491–499. (doi:10.1007/s00338-008-0375-6)
 33. Schneider K, Erez J. 2006 The effect of carbonate chemistry on calcification and photosynthesis in the hermatypic coral *Acropora eurystroma*. *Limnol. Oceanogr.* **51**, 1284–1293. (doi:10.4319/lo.2006.51.3.1284)
 34. Renegar DA, Riegl BM. 2005 Effect of nutrient enrichment and elevated CO₂ partial pressure on growth rate of Atlantic scleractinian coral *Acropora cervicornis*. *Mar. Ecol. Prog. Ser.* **293**, 69–76. (doi:10.3354/meps293069)
 35. Jokiel PL, Rodgers KS, Kuffner IB, Andersson AJ, Cox EF, Mackenzie FT. 2008 Ocean acidification and calcifying reef organisms: a mesocosm investigation. *Coral Reefs* **27**, 473–483. (doi:10.1007/s00338-008-0380-9)
 36. Reynaud S, Leclercq N, Romaine-Lioud S, Ferrier-Pagès C, Jaubert J, Gattuso J-P. 2003 Interacting effects of CO₂ partial pressure and temperature on photosynthesis and calcification in a scleractinian coral. *Glob. Change Biol.* **9**, 1660–1668. (doi:10.1046/j.1365-2486.2003.00678.x)
 37. Cohen A, Holcomb M. 2009 Why corals care about ocean acidification: uncovering the mechanism. *Oceanography* **22**, 118–127. (doi:10.5670/oceanog.2009.102)
 38. Rodolfo-Metalpa R, Martin S, Ferrier-Pages C, Gattuso JEANP. 2010 Response of the temperate coral *Cladocora caespitosa* to mid-and long-term exposure to pCO₂ and temperature levels projected for the year 2100 AD. *Biogeoscience* **7**, 289–300. (doi:10.5194/bg-7-289-2010)
 39. Holcomb M, McCorkle DC, Cohen AL. 2010 Long-term effects of nutrient and CO₂ enrichment on the temperate coral *Astrangia poculata* (Ellis and Solander, 1786). *J. Exp. Mar. Biol. Ecol.* **386**, 27–33. (doi:10.1016/j.jembe.2010.02.007)
 40. Rodolfo-Metalpa R *et al.* 2011 Coral and mollusc resistance to ocean acidification adversely affected by warming. *Nat. Clim. Change* **1**, 308–312. (doi:10.1038/nclimate1200)
 41. Edmunds PJ. 2011 Zooplanktivory ameliorates the effects of ocean acidification on the reef coral *Porites* spp. *Limnol. Oceanogr.* **56**, 2402–2410. (doi:10.4319/lo.2011.56.6.2402)
 42. Muehllehner N, Edmunds PJ. 2008 Effects of ocean acidification and increased temperature on skeletal growth of two scleractinian corals, *Pocillopora meandrina* and *Porites rus*. In *Proc. of the 11th Int. Coral Reef Symp.*, pp. 57–61. Fort Lauderdale, FL: International Coral Reef Symposium (ICRS).

43. Veron J, Stafford-Smith M. 2000 *Corals of the world*, p. 463. Townsville, SC: Australian Institute of Marine Sciences.
44. Atkinson MJ, Bingman C. 1998 Elemental composition of commercial seasalts. *J. Aquaculture Aquat. Sci.* **8**, 39–43.
45. Castillo KD, Helmuth BST. 2005 Influence of thermal history on the response of *Montastraea annularis* to short-term temperature exposure. *Mar. Biol.* **148**, 261–270. (doi:10.1007/s00227-005-0046-x)
46. Castillo K, Lima F. 2010 Comparison of *in situ* and satellite-derived (MODIS-Aqua/Terra) methods for assessing temperatures on coral reefs. *Limnol. Oceanogr. Methods* **8**, 107–117. (doi:10.4319/lom.2010.8.0107)
47. Hofmann GE *et al.* 2011 High-frequency dynamics of ocean pH: a multi-ecosystem comparison. *PLoS ONE* **6**, e28983. (doi:10.1371/journal.pone.0028983)
48. Dickson A, Sabine C, Christian J. 2007 *Guide to best practices for ocean CO₂ measurements*. Sidney, Canada: PICES Special Publication 3.
49. Lewis E, Wallace D. 1998 *CO₂SYS: program developed for CO₂ system calculations, ORNL/CDIAC-105*. Oak Ridge, TN: Oak Ridge National Laboratory, US Department of Energy.
50. Roy R, Roy L, Vogel K, Porter-Moore C, Pearson T, Good C, Millero FJ, Campbell D. 1993 The dissociation constants of carbonic acid in seawater at salinities 5 to 45 and temperatures 0 to 45°C. *Mar. Chem.* **44**, 249–267. (doi:10.1016/0304-4203(93)90207-5)
51. Mucci A. 1983 The solubility of calcite and aragonite in seawater at various salinities, temperatures, and one atmosphere total pressure. *Am. J. Sci.* **283**, 780–799. (doi:10.2475/ajs.283.7.780)
52. Spencer Davies P. 1989 Short-term growth measurements of corals using an accurate buoyant weighing technique. *Mar. Biol.* **101**, 389–395. (doi:10.1007/BF00428135)
53. Bates D, Martin M, Ben B, Walker S. 2014 *lme4: Linear mixed effects models using Eigen and S4*. (R package v. 1.0–6). See <http://CRAN.R-project.org/package=lme4>.
54. R Development Core Team. 2014 *R: a language and environment for statistical computing*. Vienna, Austria: R Foundation for Statistical Computing.
55. Baguley T. 2012 Calculating and graphing within-subject confidence intervals for ANOVA. *Behav. Res. Methods* **44**, 158–175. (doi:10.3758/s13428-011-0123-7)
56. Baguley T. 2012 *Serious stats: a guide to advanced statistics for the behavioral sciences*. Basingstoke, UK: Palgrave.
57. Form AU, Riebesell U. 2012 Acclimation to ocean acidification during long-term CO₂ exposure in the cold-water coral *Lophelia pertusa*. *Glob. Change Biol.* **18**, 843–853. (doi:10.1111/j.1365-2486.2011.02583.x)
58. Frade PR, Bongaerts P, Winkelhagen AJS, Tonk L, Bak RPM. 2008 In situ photobiology of corals over large depth ranges: a multivariate analysis on the roles of environment, host, and algal symbiont. *Limnol. Oceanogr.* **53**, 2711–2723. (doi:10.4319/lo.2008.53.6.2711)
59. Brading P, Warner ME, Davey P, Smith DJ, Achterberg EP, Suggett DJ. 2011 Differential effects of ocean acidification on growth and photosynthesis among phylogenotypes of *Symbiodinium* (Dinophyceae). *Limnol. Oceanogr.* **56**, 927–938. (doi:10.4319/lo.2011.56.3.0927)
60. Brading P, Warner ME, Smith DJ, Suggett DJ. 2013 Contrasting modes of inorganic carbon acquisition amongst *Symbiodinium* (Dinophyceae) phylogenotypes. *New Phytol.* **200**, 432–442. (doi:10.1111/nph.12379)
61. Crawley A, Kline DI, Dunn S, Anthony KEN, Dove S. 2010 The effect of ocean acidification on symbiotic photorespiration and productivity in *Acropora formosa*. *Glob. Change Biol.* **16**, 851–863. (doi:10.1111/j.1365-2486.2009.01943.x)
62. McCulloch M, Falter J, Trotter J, Montagna P. 2012 Coral resilience to ocean acidification and global warming through pH up-regulation. *Nat. Clim. Change* **2**, 623–627. (doi:10.1038/nclimate1473)
63. Ries JB. 2011 A physicochemical framework for interpreting the biological calcification response to CO₂-induced ocean acidification. *Geochim. Cosmochim. Acta* **75**, 4053–4064. (doi:10.1016/j.gca.2011.04.025)
64. Venn AA, Tambutté E, Holcomb M, Laurent J, Allemand D, Tambutté S. 2013 Impact of seawater acidification on pH at the tissue–skeleton interface and calcification in reef corals. *Proc. Natl Acad. Sci. USA* **110**, 1634–1639. (doi:10.1073/pnas.1216153110)
65. Al-Horani FA, Al-Moghrabi SM, de Beer D. 2003 The mechanism of calcification and its relation to photosynthesis and respiration in the scleractinian coral *Galaxea fascicularis*. *Mar. Biol.* **142**, 419–426. (doi:10.1007/s00227-002-0981-8)
66. Venn A, Tambutté E, Holcomb M, Allemand D, Tambutté S. 2011 Live tissue imaging shows reef corals elevate pH under their calcifying tissue relative to seawater. *PLoS ONE* **6**, e20013. (doi:10.1371/journal.pone.0020013)
67. Trotter J *et al.* 2011 Quantifying the pH ‘vital effect’ in the temperate zooxanthellate coral *Cladocora caespitosa*: validation of the boron seawater pH proxy. *Earth Planet. Sci. Lett.* **303**, 163–173. (doi:10.1016/j.epsl.2011.01.030)
68. Anagnostou E, Huang KF, You CF, Sikes EL, Sherrell RM. 2012 Evaluation of boron isotope ratio as a pH proxy in the deep sea coral *Desmophyllum dianthus*: evidence of physiological pH adjustment. *Earth Planet. Sci. Lett.* **349–350**, 251–260. (doi:10.1016/j.epsl.2012.07.006)
69. Cohen A, McCorkle D, de Putron S, Rose KA. 2009 Morphological and compositional changes in the skeletons of new coral recruits reared in acidified seawater: insights into the biomineralization response to ocean acidification. *Geochem. Geophys. Geosyst.* **10**, Q07005. (doi:10.1029/2009GC002411)
70. McCulloch M *et al.* 2012 Resilience of cold-water scleractinian corals to ocean acidification: boron isotopic systematics of pH and saturation state up-regulation. *Geochim. Cosmochim. Acta* **87**, 21–34. (doi:10.1016/j.gca.2012.03.027)
71. Holcomb M, Venn AA, Tambutte E, Tambutte S, Allemand D, Trotter J, McCulloch M. 2014 Coral calcifying fluid pH dictates response to ocean acidification. *Sci. Rep.* **4**, 5207. (doi:10.1038/srep05207)
72. Huey RB, Kingsolver JG. 1989 Evolution of thermal sensitivity of ectotherm performance. *Trends Ecol. Evol.* **4**, 131–135. (doi:10.1016/0169-5347(89)90211-5)
73. Pörtner HO *et al.* 2006 Trade-offs in thermal adaptation: the need for a molecular to ecological integration. *Physiol. Biochem. Zool.* **79**, 295–313. (doi:10.1086/499986)
74. Angilletta MJ. 2009 *Thermal adaptation, a theoretical and empirical synthesis*. Oxford, UK: Oxford University Press.
75. Hochachka P, Somero G. 2002 *Biochemical adaptations: mechanism and process in physiological evolution*. New York, NY: Oxford University Press.
76. Saxby T, Dennison WC, Hoegh-Guldberg O. 2003 Photosynthetic responses of the coral *Montipora digitata* to cold temperature stress. *Mar. Ecol. Prog. Ser.* **248**, 85–97. (doi:10.3354/meps248085)
77. Moya A, Ferrier-Pagès C, Furla P, Richier S, Tambutté E, Allemand D, Tambutté S. 2008 Calcification and associated physiological parameters during a stress event in the scleractinian coral *Stylophora pistillata*. *Comp. Biochem. Physiol. A Mol. Integr. Physiol.* **151**, 29–36. (doi:10.1016/j.cbpa.2008.05.009)
78. Chisholm JRM, Gattuso J-P. 1991 Validation of the alkalinity anomaly technique for investigating calcification and photosynthesis in coral reef communities. *Limnol. Oceanogr.* **36**, 1232–1239. (doi:10.4319/lo.1991.36.6.1232)
79. Murillo LJA, Jokiel PL, Atkinson MJ. 2014 Alkalinity to calcium flux ratios for corals and coral reef communities: variances between isolated and community conditions. *Peer J.* **2**, e249. (doi:10.7717/peerj.249)
80. Riebesell U, Fabry VJ, Hansson L, Gattuso J-P. (eds) 2010 *Guide to best practices for ocean acidification research and data reporting*, p. 260. Luxembourg: Publication Office of the European Union.
81. Cubasch U, Wuebbles D, Chen D, Facchini M, Frame D, Mahowald D, Winther J-G. 2013 Contribution of Working Group I to the Fifth Assessment Report of the Intergovernmental Panel on Climate Change. In *Climate Change 2013: The Physical Science Basis* (eds TF Stocker, D Qin, G-K Plattner, M Tignor, SK Allen, J Boschung, A Nauels, Y Xia, V Bex, PM Midgley), pp. 119–158. UK and New York, NY, USA: Cambridge University Press.

Electronic Supplementary Material for “*The reef-building coral Siderastrea siderea exhibits parabolic responses to ocean acidification and warming*”

Karl D. Castillo, Justin B. Ries, John F. Bruno, and Isaac T. Westfield

Description of coral collection sites

Forereef and backreef colonies were collected from the seaward and landward sides, respectively, of the barrier reef’s crest, approximately 40 km west of the Belize coast in the Sapodilla Cayes Marine Reserve. Nearshore *S. siderea* colonies were obtained from fringing reefs within 10 km of the Belize coast in the Port Honduras Marine Reserve. Coral colonies were collected from sites at least 0.2 km apart in order to randomize microenvironmental and genetic effects. Required permits were obtained from the Belize Fisheries Department and all corals were collected pursuant to local, federal, and international regulations.

Quantification of light conditions

Photosynthetically active radiation (PAR) in the tanks was measured beneath the plexiglass cover using a *LI-1400* datalogger affixed with a *LI-192* underwater quantum sensor (*LI-COR*; Lincoln, Nebraska; see figure S2). PAR measurements in the field were performed across nearshore, backreef, and forereef collection sites during late May and early June of multiple years and ranged from 200 to 600 $\mu\text{mol photons m}^{-2} \text{ s}^{-1}$ at 3-5 meters depth. In addition, light intensity was recorded every 15 min using *HOBO Pendant* light dataloggers (*Onset Computer Corp.*; Bourne, Massachusetts; figure S1). The light dataloggers were cleaned regularly to minimize fouling. PAR was estimated from light intensity (lux) using the equation: $1 \mu\text{mol photons (400:700 nm) m}^{-2} \text{ s}^{-1} = 51.2 \text{ lux (sensu}^{1,2})$. This light conversion was validated by mid-day measurements with the *LI-192* quantum sensor. Both the *HOBO* and *LI-192* light meters

reveal that PAR values were often higher at offshore (forereef and backreef) sites compared to nearshore sites, with nearshore values generally falling within 100 to 400 $\mu\text{mol photons m}^{-2} \text{ s}^{-1}$ because of suspended materials within the water column. This trend was more pronounced during the rainy season, which extends from June to November off the coast of southern Belize, which can receive more than 4 m of rain annually. A conservative irradiation corresponding to the average 3-5 m deep nearshore values of 250 $\mu\text{mol photons m}^{-2} \text{ s}^{-1}$ was employed in order to minimize potential light stress.

Measurement and calculation of carbonate system parameters

Temperature within the experimental tanks was measured every other day with a NIST-calibrated partial-immersion organic-filled glass thermometer (precision $\pm 0.3\%$, accuracy $\pm 0.4\%$). Salinity was measured every other day with a *YSI* 3200 conductivity meter with a *YSI* 3440 cell ($K=10$) calibrated with seawater standards (A. Dickson, Scripps Institute of Oceanography). Seawater pH was measured every other day with a *Thermo Scientific Orion 2 Star* benchtop pH meter with an *Orion* 9156BNWP pH probe, calibrated with 7.00 and 10.01 *Orion* NBS buffers traceable to NIST standard reference material (for slope of the calibration curve) and with seawater standards of known pH (A. Dickson, Scripps Institute of Oceanography; for y-intercept of the calibration curve). Seawater dissolved inorganic carbon (DIC) was measured via coulometry (*UIC 5400*) and total alkalinity (TA) was measured via closed-cell potentiometric Gran titration calibrated with certified Dickson TA/DIC standards (see Tables S1 and S2; Figures S3 and S4 for seawater chemistry data). Measurement of DIC and TA of the certified reference materials (CRMs) were consistently within 0.3% of certified values.

Differences between the measured and certified TA and DIC values of the CRMs were used to correct measurements of experimental seawater solutions.

Seawater $p\text{CO}_2$, pH, carbonate ion concentration ($[\text{CO}_3^{2-}]$), bicarbonate ion concentration ($[\text{HCO}_3^-]$), aqueous CO_2 , and aragonite saturation state (Ω_A) were calculated from measured DIC, TA, temperature and salinity with the program CO_2SYS ³, using values for K_1 and K_2 carbonic acid constants ⁴, the stoichiometric aragonite solubility product ⁵, and an atmospheric pressure of 1.015 atm. Temporal variability in the prescribed carbonate system parameters throughout the duration of the experiments were generally consistent with that reported for natural reefs ⁶.

Empirical derivation of the buoyant weight-dry weight relationship

Siderastrea siderea specimens were weighed at the beginning of the experiment and approximately every 30 days thereafter, with the final measurement obtained at 95 days. Each coral specimen was suspended by aluminum wire from a *Cole-Parmer* bottom-loading scale (precision ± 0.001 ; accuracy ± 0.002) at 10 cm depth in a tank filled with experimental seawater maintained at 25 °C and salinity of 33. A plastic-coated zinc mass standard was intermittently weighed to ensure consistency of the buoyant weight method.

The buoyant weight-dry weight relationship for the coral *S. siderea* was empirically derived by plotting the final dry weights (after removal of organic matter) against the final buoyant weights of 60 coral specimens randomly selected from the four $p\text{CO}_2$ (324, 477, 604, 2553 μatm) and the three temperature (25, 28, 32 °C) treatments employed in the experiments (Figure S5). The observation that specimens from all treatments are highly correlated ($R^2 = 0.9985$, $p < 0.001$) and fall on approximately the same line indicates that the density of the coral

skeletons does not vary appreciably amongst treatments. Thus, a single linear equation can be used to convert buoyant weight to dry weight for the purposes of estimating net calcification rates:

$$\text{Dry weight (mg)} = 1.5567 * \text{Buoyant weight (mg)} + 1.1235.$$

Additional explanations of the statistical model employed

Hierarchical mixed-effects models were employed to account for the combined repeated-measures/split-plot design. Each coral's measured dry weight (mg) was divided by its initial surface area (cm²) to yield a normalized weight (mg cm⁻²). In the *p*CO₂ and temperature experiments, two different response variables were analyzed separately. Firstly, normalized dry weight (mg cm⁻²) was regressed against continuous time and treatment to assess the overall effect of treatment on *S. siderea* calcification rates for the 95-day experiments. This approach yields a coefficient of time in the regression model and the extent to which it varies by treatment. Normalized calcification rate (mg cm⁻² d⁻¹) was then obtained by extracting the regression coefficient of the continuous time variable in the model. Secondly, normalized calcification rates of each coral were assessed across three discrete observational intervals and regressed against treatment and time in order to assess the impact of treatment duration on coral calcification response to warming and acidification (see electronic supplementary material, tables S3 and S4). Difference-adjusted-confidence-intervals were used to reveal statistically significant differences amongst *p*CO₂ and temperature treatments^{7,8}.

In the combined repeated-measures/split-plot design, tanks represent plots, and temperature and *p*CO₂ represent whole-plot treatments, while reef zones of coral colonies represent split-plot treatments. Random effects at the colony level were employed to account for

the grouping of corals by colony (genotype), and at the level of the individual coral specimen to account for repeated measures. Repeated measures are nested in coral units, which are nested in colony blocks and tank blocks, with tank and colony blocks crossed.

The full interaction model was fit using restricted maximum likelihood to obtain unbiased estimates of the variance components and parameter standard errors. The variance components of the model varied as the predictors of the model were fixed. AIC was used to determine which level-1 coefficients should be randomized at each level. The AIC-best random effects model was refit using the Satterthwaite approximation in *SAS/STAT* software (Version 9.3 of the *SAS* System for Windows⁹) to evaluate statistical significance of individual model terms. Finally, Bayesian methods were employed to obtain Bayesian-credible and highest-probability density intervals for model parameters of interest. Markov chain Monte Carlo estimation of the Bayesian models was performed using *JAGS* 3.1.0¹⁰.

Estimation of photosynthetic rates. One-time measurements of the maximum photosynthetic efficiency of photosystem II (F_v/F_m ; where $F_v = F_m - F_o$; and F_v , F_m , and F_o are variable, maximum, and minimum fluorescence, respectively) were obtained on day 94 of the experiments with an underwater PAM fluorometer (saturation width 0.80 s of $> 5000 \mu\text{mol photon m}^{-2} \text{s}^{-1}$ saturation light pulse; *Diving-PAM*, Walz, Germany) at 20:00 hours, two hours after daytime illumination ended to ensure that non-photochemical quenching was suppressed and that the corals were adequately dark-adapted. Measured F_v/F_m was converted to maximum photosynthetic rate (ETR_{max}) using the approximately linear relationship between F_v/F_m and ETR_{max} estimated from data reported in Frade et al. (2008)¹¹ ($\text{ETR}_{\text{max}} = -186.08*(F_v/F_m) + 172.64$; $R^2 = 0.2553$; linear regression without outlier in figure S6; table S11)—the only

published dataset that the authors were able to identify that contained simultaneous measurements of F_v/F_m and maximum photosynthetic rate (ETR_{max}) for multiple species of tropical scleractinian corals across a range of light conditions.

Supplementary Tables and Figures

Table S1. Average calculated and measured parameters for $p\text{CO}_2$ treatments: $p\text{CO}_2$ of the mixed gases in equilibrium with the experimental seawaters ($p\text{CO}_2(\text{gas-e})$); calculated pH (pH_c); carbonate ion concentration ($[\text{CO}_3^{2-}]$); bicarbonate ion concentration ($[\text{HCO}_3^-]$); dissolved carbon dioxide ($[\text{CO}_2]_{\text{sw}}$); and aragonite saturation state (Ω_A); temperature (T); salinity (Sal), measured pH (pH_m), total alkalinity (TA), and dissolved inorganic carbon (DIC). “SE” is the standard error of the mean, “SD” is the standard deviation of the mean, and “ n ” is the sample size.

<i>Calculated parameters</i>					
$p\text{CO}_2(\text{gas-e})$	(μatm)	324	477	604	2553
	SD	89	83	107	506
	SE	14	13	17	78
	Range	125 - 487	356 - 615	418 - 812	1500 - 3364
	n	42	42	42	42
pH_c		8.07	7.90	7.82	7.32
	SD	0.12	0.13	0.13	0.14
	SE	0.02	0.02	0.02	0.02
	Range	7.81 - 8.23	7.62 - 8.05	7.48 - 7.96	6.99 - 7.49
	n	42	42	42	42
$[\text{CO}_3^{2-}]$	(μM)	246	176	155	66
	SD	94	66	60	26
	SE	15	10	9	4
	Range	85 - 372	55 - 270	38 - 232	18 - 100
	n	42	42	42	42
$[\text{HCO}_3^-]$	(μM)	1480	1516	1605	2133
	SD	378	320	405	408
	SE	58	49	63	63
	Range	825 - 1993	883 - 1969	896 - 2254	1318 - 2620
	n	42	42	42	42
$[\text{CO}_2]_{\text{sw}}$	(μM)	8.5	12.5	15.9	67.2
	SD	2.4	2.2	2.8	13.2
	SE	0.4	0.3	0.4	2.0
	Range	3.2 - 12.9	9.4 - 16.0	11.0 - 21.3	39.6 - 88.6

	n	42	42	42	42
Ω_A		4.0	2.8	2.5	1.1
	SD	1.5	1.1	1.0	0.4
	SE	0.2	0.2	0.1	0.1
	Range	1.4 - 6.0	0.9 - 4.3	0.6 - 3.7	0.3 - 1.6
	n	42	42	42	42
<i>Measured parameters</i>					
T	(°C)	28.14	28.16	28.04	27.93
	SD	0.27	0.24	0.28	0.19
	SE	0.03	0.02	0.03	0.02
	Range	27.70 - 28.80	27.80 - 28.90	27.50 - 28.90	27.60 - 28.50
	n	108	108	108	108
Sal		35.04	35.01	35.11	35.04
	SD	0.30	0.30	0.37	0.30
	SE	0.03	0.03	0.03	0.03
	Range	34.50 - 35.70	34.50 - 35.70	34.10 - 35.80	34.20 - 35.70
	n	108	108	108	108
pH _m		8.05	7.93	7.83	7.35
	SD	0.17	0.12	0.14	0.13
	SE	0.01	0.01	0.01	0.01
	Range	7.84 - 8.52	7.76 - 8.36	7.62 - 8.24	7.21 - 7.72
	n	108	108	108	108
TA	(μ M)	2086	1951	1986	2291
	SD	554	458	532	458
	SE	85	71	82	71
	Range	1124 - 2702	1088 - 2601	1015 - 2760	1372 - 2786
	n	42	42	42	42
DIC	(μ M)	1735	1704	1776	2266
	SD	459	381	463	428
	SE	71	59	72	66
	Range	937 - 2301	964 - 2249	956 - 2489	1412 - 2778
	n	42	42	42	42

Table S2. Average measured and calculated parameters for temperature treatments: temperature (T); salinity (Sal); measured pH (pH_m); total alkalinity (TA); dissolved inorganic carbon (DIC); *p*CO₂ of the mixed gases in equilibrium with the experimental seawaters [*p*CO₂ (gas-e)]; pH (pH_c); carbonate ion concentration ([CO₃²⁻]); bicarbonate ion concentration ([HCO₃⁻]); dissolved carbon dioxide ([CO₂]_{sw}); and aragonite saturation state (Ω_A). “SE” is the standard error of the mean, “SD” is the standard deviation of the mean, and “*n*” is the sample size.

<i>Measured parameters</i>				
T	(°C)	25.01	28.16	32.01
	SD	0.17	0.24	0.17
	SE	0.01	0.02	0.02
	Range	24.70 - 25.50	27.80 - 28.90	31.60 - 32.40
	n	108	108	108
Sal		34.97	35.01	35.20
	SD	0.30	0.29	0.32
	SE	0.03	0.03	0.03
	Range	34.40 - 35.90	34.50 - 35.70	34.40 - 36.20
	n	108	108	108
pH _m		7.93	7.93	8.11
	SD	0.10	0.13	0.07
	SE	0.01	0.01	0.01
	Range	7.86 - 8.27	7.76 - 8.36	8.09 - 8.42
	n	108	108	108
TA	(μM)	2097	1951	2725
	SD	448	458	446
	SE	69	71	69
	Range	1222 - 2728	1088 - 2601	1675 - 3217
	n	42	42	42
DIC	(μM)	1859	1704	2284
	SD	369	381	344
	SE	57	59	53
	Range	1145 - 2392	964 - 2249	1491 - 2683
	n	42	42	42
<i>Calculated parameters</i>				

$p\text{CO}_2$ (gas-e)	(μatm)	515	477	472
	SD	92	83	86
	SE	14	13	13
	Range	365 - 694	356 - 615	319 - 694
	n	42	42	42
<hr/>				
pH _c		7.90	7.90	8.03
	SD	0.13	0.12	0.11
	SE	0.02	0.02	0.02
	Range	7.59 - 8.04	7.62 - 8.05	7.70 - 8.15
	n	42	42	42
<hr/>				
$[\text{CO}_3^{2-}]$	(μM)	175	176	336
	SD	67	66	93
	SE	10	10	14
	Range	52 - 263	55 - 270	113 - 463
	n	42	42	42
<hr/>				
$[\text{HCO}_3^-]$	(μM)	1669	1516	1936
	SD	307	320	263
	SE	47	49	41
	Range	1072 - 2118	883 - 1969	1350 - 2313
	n	42	42	42
<hr/>				
$[\text{CO}_2]$ (sw)	(μM)	14.6	12.5	11.3
	SD	2.6	2.2	2.0
	SE	0.4	0.3	0.3
	Range	10.3 - 19.6	9.4 - 16.0	7.6 - 16.5
	n	42	42	42
<hr/>				
Ω_A		2.8	2.8	5.5
	SD	1.1	1.1	1.5
	SE	0.2	0.2	0.2
	Range	0.8 - 4.2	0.9 - 4.3	1.9 - 7.6
	n	42	42	42

Table S3. Observational intervals for *S. siderea* corals reared at the four $p\text{CO}_2$ treatments levels. Buoyant weighing of the coral specimens was conducted over consecutive days, causing observational intervals to vary by a few days for corals in the different $p\text{CO}_2$ treatments. To account for variability in the duration of these observational intervals, changes in corals' surface-area-normalized dry weights (mg cm^{-2}) were divided by the exact duration of their observational interval, thus yielding average daily calcification rates ($\text{mg cm}^{-2} \text{d}^{-1}$).

Cohort	$p\text{CO}_2$ Treatment Tanks	Observation Interval			Number of Corals	Percent of Sample
		1 st	2 nd	3 rd		
1	324 μatm (tanks 1-3) 604 μatm (tank 3)	[0,35] 35 days	[35, 60] 25 days	[60, 95] 35 days	72	33.3
2	477 μatm (tanks 1-3)	[0,34] 34 days	[34, 60] 26 days	[60, 96] 34 days	54	25.0
3	604 μatm (tanks 1 and 2)	[0,35] 35 days	[35, 60] 25 days	[60, 95] 35 days	36	16.7
4	2553 μatm (tanks 1-3)	[0,33] 33 days	[33, 60] 27 days	[60,94] 34 days	54	25.0

Table S4. Observational intervals for *S. siderea* corals reared at the three temperature levels. Buoyant weighing of the coral specimens was conducted over consecutive days, causing observational intervals to vary by a few days for corals in the different temperature treatments. To account for variability in the duration of these observational intervals, changes in corals' surface-area-normalized dry weights (mg cm^{-2}) were divided by the exact duration of their observational interval, thus yielding average daily calcification rates ($\text{mg cm}^{-2} \text{d}^{-1}$).

Cohort	Temperature Treatment Tanks	Observation Interval			Number of Corals	Percent of Sample
		1 st	2 nd	3 rd		
1	25 °C (tanks 1-3)	[0, 35] 35 days	[35, 60] 25 days	[60, 94] 34 days	54	33.3
2	28 °C (tanks 1-3)	[0, 34] 34 days	[34, 60] 26 days	[60, 96] 36 days	54	33.3
3	32 °C (tanks 1-3)	[0, 35] 35 days	[35, 60] 25 days	[60, 95] 35 days	54	33.3

Table S5. Summary of mixed effects model to examine differences in calcification rates across $p\text{CO}_2$ treatments with reefzone removed as a factor: covariance parameter estimates for random effects (a); Type 1 test of fixed effects using sequential variables-added-in-order-test (b); solutions for fixed effects (c); and 95% interval estimates of $p\text{CO}_2$ -time interaction effects in which 324 μatm is the reference group (d). Confidence intervals are obtained using Satterwaite correction and Bayesian model with uninformative priors using Markov chain Monte Carlo estimation. 95% credible intervals and highest posterior density intervals are shown.

(a)

Covariance Parameter	Subject	Estimate
(Intercept)	Coral ID	0.04582
Total Time	Coral ID	0.08666
(Intercept)	Colony	0.01859
Total Time	Colony	0.1658
Total Time	Tank	0.07877
Residual		0.000159

(b)

Parameter	Num DF	Den DF	<i>F-value</i>	<i>p-value</i>
Total Time	1	22.5	291.21	<0.0001
$p\text{CO}_2$	3	198	2.34	0.0744
Total Time: $p\text{CO}_2$	6	8.01	4.33	0.0433

(c)

Parameter	$p\text{CO}_2$	Estimate	SE	DF	t -value	p -value
(Intercept)		1.1867	0.04340	38.5	27.35	<0.0001
Total Time		1.9004	0.1941	13.3	9.79	<0.0001
$p\text{CO}_2$	2553	0.06985	0.04136	196	1.69	0.0928
$p\text{CO}_2$	604	-0.06720	0.04153	197	-1.62	0.1072
$p\text{CO}_2$	477	-0.04390	0.04136	196	-1.06	0.2898
$p\text{CO}_2$	324	0
Total Time: $p\text{CO}_2$	2553	-0.02260	0.2387	8.01	-0.09	0.9269
Total Time: $p\text{CO}_2$	604	0.6080	0.2387	8.02	2.55	0.0343
Total Time: $p\text{CO}_2$	477	0.5848	0.2386	8	2.45	0.0399
Total Time: $p\text{CO}_2$	324	0

(d)

Interaction Effect	Bayesian Credible Intervals	Bayesian HPD Intervals
324 μatm	reference	reference
477 μatm	(0.009, 1.173)	(0.008, 1.173)
604 μatm	(0.015, 1.183)	(0.013, 1.175)
2800 μatm	(-0.638, 0.556)	(-0.633, 0.561)

Note: Intervals that do not include “zero” are significant.

Table S6. Summary of mixed effects model to examine differences in calcification rates across temperature treatments with reefzone removed as a factor: covariance parameter estimates for random effects (a); Type 1 test of fixed effects using sequential variables-added-in-order-test (b); solutions for fixed effects (c); and 95% interval estimates of $p\text{CO}_2$ -time interaction effects in which 25 °C is the reference group (d). Confidence intervals are obtained using Satterwaite correction and Bayesian model with uninformative priors using Markov chain Monte Carlo estimation. 95% credible intervals and highest posterior density intervals are shown.

(a)

Covariance Parameter	Subject	Estimate
(Intercept)	Coral ID	0.04857
Total Time	Coral ID	0.07724
(Intercept)	Colony	0.009733
Total Time	Colony	0.07415
(Intercept)	Tank	0.000142
Total Time	Tank	0.05139
Residual		0.000144

(b)

Parameter	Num DF	Den DF	<i>F-value</i>	<i>p-value</i>
Total Time	1	13.6	249.42	<0.0001
Temperature	2	6.45	0.66	0.5469
Total Time: Temperature	2	6.01	55.01	0.0001

(c)

Parameter	Temperature	Estimate	SE	DF	<i>t-value</i>	<i>p-value</i>
(Intercept)		1.2141	0.03879	11.8	31.30	<0.0001
Total Time		1.8958	0.1526	8.71	12.42	<0.0001
Temperature	32	0.06170	0.04372	5.96	1.41	0.2082
Temperature	28	-0.07456	0.04366	5.93	-1.71	0.1392
Temperature	25	0
Total Time: Temp	32	-1.4150	0.1956	6.02	-7.23	0.0003
Total Time: Temp	28	0.5795	0.1956	6.01	2.96	0.0251
Total Time: Temp	25	0

(d)

Interaction Effect	Bayesian Credible Intervals	Bayesian HPD Intervals
25°C	reference	reference
28°C	(0.037, 1.115)	(0.015, 1.093)
32°C	(-1.948, -0.881)	(-1.949, -0.881)

Note: Intervals that do not include “zero” are significant.

Table S7. Summary of mixed-effects model to examine differences in calcification rates across temperature treatments with reefzone removed as a factor: covariance parameter estimates for random effects (a); Type 1 test of fixed effects using sequential variables-added-in-order-test (b); and solutions for fixed-effects (c).

(a)

Covariance Parameter	Subject	Estimate
(Intercept)	Coral ID	0.05091
(Intercept)	Colony	0.16370
(Intercept)	Tank	0.07557
Residual		0.19270

(b)

Parameter	Num DF	Den DF	<i>F-value</i>	<i>p-value</i>
Time	2	424	127.48	<0.0001
<i>p</i> CO ₂	3	8.01	4.50	0.0394
Time: <i>p</i> CO ₂	6	424	16.08	<0.0001

(c)

Parameter	$p\text{CO}_2$	Time	Estimate	SE	DF	<i>t-value</i>	<i>p-value</i>
(Intercept)			1.4781	0.1970	15.2	7.50	<0.0001
Time		90	0.4803	0.08448	424	5.69	<0.0001
Time		60	0.7510	0.08448	424	8.89	<0.0001
Time		30	0
$p\text{CO}_2$	2553		0.3115	0.2438	9.46	1.28	0.2319
$p\text{CO}_2$	604		0.6523	0.2439	9.47	2.67	0.0244
$p\text{CO}_2$	477		0.4321	0.2438	9.46	1.77	0.1085
$p\text{CO}_2$	324		0
Time: $p\text{CO}_2$	2553	90	-0.5025	0.1195	424	-4.21	<0.0001
Time: $p\text{CO}_2$	2553	60	-0.5476	0.1195	424	-4.58	<0.0001
Time: $p\text{CO}_2$	2553	30	0
Time: $p\text{CO}_2$	604	90	-0.3066	0.1195	424	-2.57	0.0106
Time: $p\text{CO}_2$	604	60	0.1844	0.1195	424	1.54	0.1234
Time: $p\text{CO}_2$	604	30	0
Time: $p\text{CO}_2$	477	90	0.3364	0.1195	424	2.82	0.0051
Time: $p\text{CO}_2$	477	60	0.05461	0.1195	424	0.46	0.6478
Time: $p\text{CO}_2$	477	30	0
Time: $p\text{CO}_2$	324	90	0
Time: $p\text{CO}_2$	324	60	0
Time: $p\text{CO}_2$	324	30	0

Table S8. Summary of mixed-effects model to examine differences in calcification rates across temperature treatments with reefzone removed as a factor: covariance parameter estimates for random effects (a); Type 1 test of fixed-effects using sequential variables-added-in-order-test (b); and solutions for fixed effects (c).

a.

Covariance Parameter	Subject	Estimate
(Intercept)	Coral ID	0.05650
(Intercept)	Colony	0.07322
(Intercept)	Tank	0.04854
Residual		0.1381

b.

Parameter	Num DF	Den DF	<i>F-value</i>	<i>p-value</i>
Time	2	318	22.56	<0.0001
Temperature	2	6.01	56.93	0.0001
Time: Temperature	4	318	67.35	<0.0001

c.

Parameter	Temperature	Time	Estimate	SE	DF	<i>t-value</i>	<i>p-value</i>
(Intercept)			1.9005	0.1546	10.2	12.30	<0.0001
Time		90	0.8167	0.07153	318	11.42	<0.0001
Time		60	0.8056	0.07153	318	11.26	<0.0001
Time		30	0
Temperature	32		-1.0620	0.1990	7.19	-5.34	0.0010
Temperature	25		-0.3174	0.1990	7.19	-1.60	0.1536
Temperature	28		0
Time: Temperature	32	90	-1.4030	0.1012	318	-13.87	<0.0001
Time: Temperature	32	60	-1.3231	0.1012	318	-13.08	<0.0001
Time: Temperature	32	30	0
Time: Temperature	25	90	-0.2520	0.1012	318	-2.49	0.0133
Time: Temperature	25	60	-0.4835	0.1012	318	-4.78	<0.0001
Time: Temperature	25	30	0
Time: Temperature	28	90	0
Time: Temperature	28	60	0
Time: Temperature	28	30	0

Table S9. Summary of mixed-effects model to examine differences in calcification rates across reefzones within $p\text{CO}_2$ treatments: covariance parameter estimates for random effects (a) and Type 1 test of fixed-effects using sequential-variables-added-in-order test (b).

(a)

Covariance Parameter	Subject	Estimate
(Intercept)	Coral ID	0.04587
Total Time	Coral ID	0.08786
(Intercept)	Colony	0.02061
Total Time	Colony	0.19000
Total Time	Tank	0.07807
Residual		0.00015

(b)

Parameter	Num DF	Den DF	<i>F-value</i>	<i>p-value</i>
Total Time	1	21.6	269.54	<0.0001
$p\text{CO}_2$	3	195	2.24	0.0846
Time: $p\text{CO}_2$	3	8.03	4.35	0.0425
Reefzone	2	15.8	0.32	0.7332
Total Time: Reefzone	2	15.1	0.01	0.9873
$p\text{CO}_2$: Reefzone	6	191	0.93	0.4724
Total Time: $p\text{CO}_2$: Reefzone	6	182	0.69	0.6585

Table S10. Summary of mixed-effects model to examine differences in calcification rates across reefzones within temperature treatments: covariance parameter estimates for random effects (a) and Type 1 test of fixed-effects using sequential-variables-added-in-order-test (b).

(a)

Covariance Parameter	Subject	Estimate
(Intercept)	Coral ID	0.04974
Total Time	Coral ID	0.07665
(Intercept)	Colony	0.01168
Total Time	Colony	0.08155
(Intercept)	Tank	0.00005
Total Time	Tank	0.05215
Residual		0.00014

(b)

Parameter	Num DF	Den DF	<i>F-value</i>	<i>p-value</i>
Total Time	1	13.7	238.40	<0.0001
Temperature	2	6.42	0.66	0.5490
Total Time: Temperature	2	6.02	54.41	0.0001
Reefzone	2	15.5	0.01	0.9921
Total Time: Reefzone	2	14.6	0.25	0.7840
Temperature: Reefzone	4	135	0.25	0.9102
Total Time: Temperature: Reefzone	4	132	1.19	0.3196

Table S11. Average measured F_v/F_m obtained on day 94 of the experiment and maximum photosynthetic rate (ETR_{max}) estimated using the approximately linear relationship between F_v/F_m and ETR_{max} ($ETR_{max} = -186.08*(F_v/F_m) + 172.64$; $R^2 = 0.2553$) from data reported in Frade et al. (2008; see Figure S6).

pCO_2 (μatm)	Mean F_v/F_m (dusk)	Maximum Photosynthetic Rate (ETR_{max} ; $\mu mol CO_2 m^{-2} s^{-1}$)
324	0.6527	51.1780
477	0.6249	56.3607
604	0.6169	57.8320
2553	0.6264	56.0746

Figure S1. Photosynthetic active radiation (PAR) measurements (December 2009 to September 2010) for offshore and nearshore sites where *Siderastrea siderea* corals were collected for the $p\text{CO}_2$ and temperature experiments.

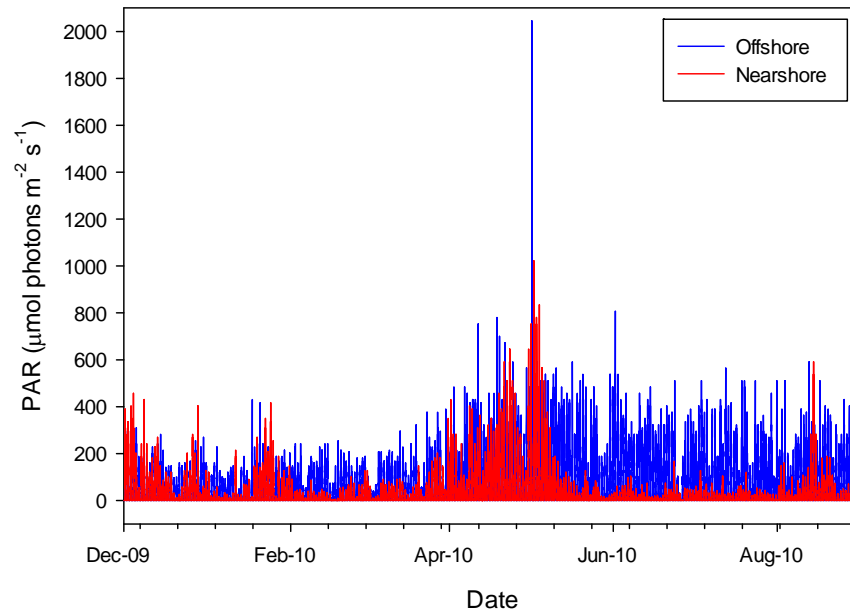


Figure S2. Twelve-hour light cycle for *Siderastrea siderea* corals maintained under the four $p\text{CO}_2$ (324, 477, 604, 2553 μatm) and the three temperature (25, 28, 32 $^\circ\text{C}$) treatments over the 95-day experimental interval.

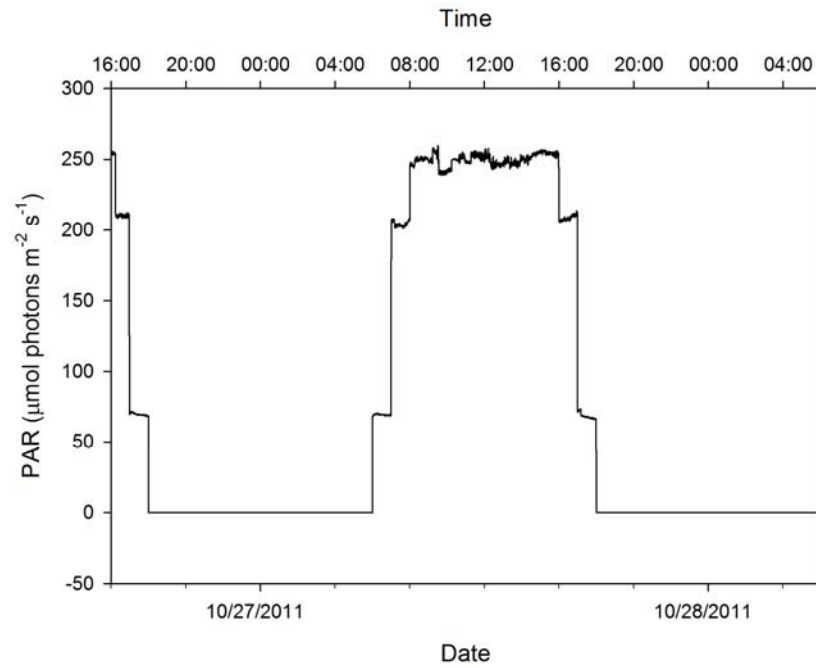
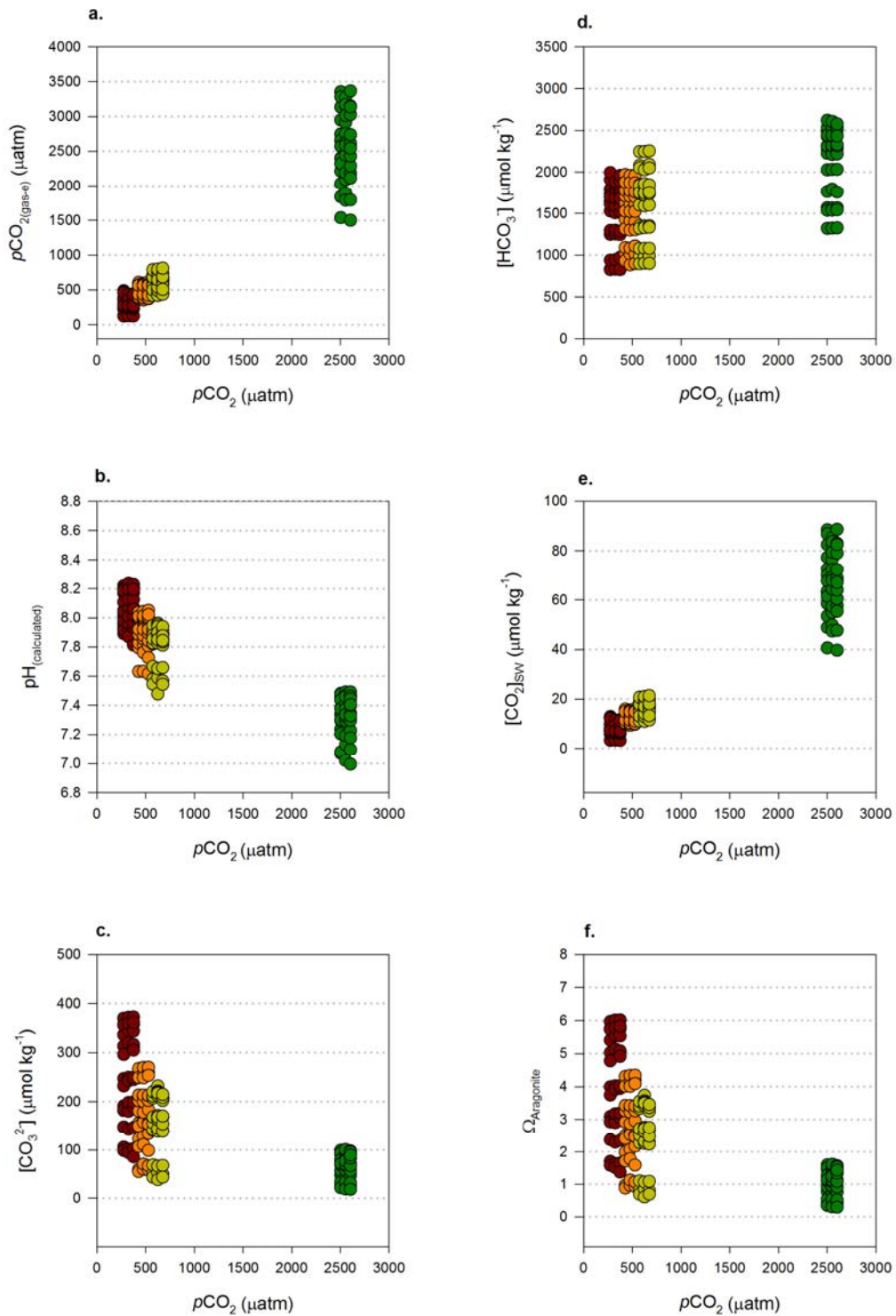


Figure S3. Calculated and measured parameters for $p\text{CO}_2$ treatments over the 95-day experimental interval: calculated $p\text{CO}_2$ of the mixed gases in equilibrium with the experimental seawaters (a); calculated pH (b); calculated carbonate ion concentration (c); calculated bicarbonate ion concentration (d); calculated dissolved carbon dioxide (e); calculated aragonite saturation state (f); measured temperature (g); measured salinity (h); measured pH (i); measured total alkalinity (j); and measured dissolved inorganic carbon (k).



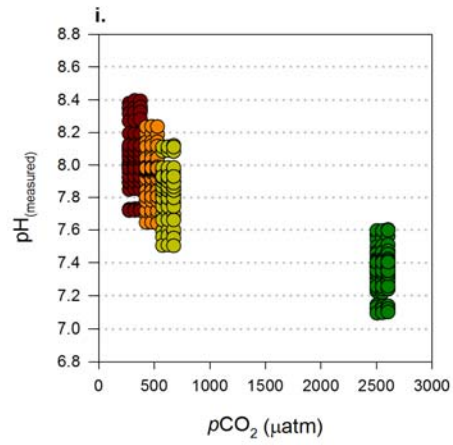
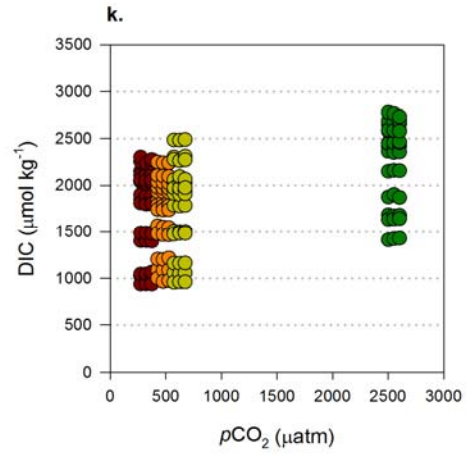
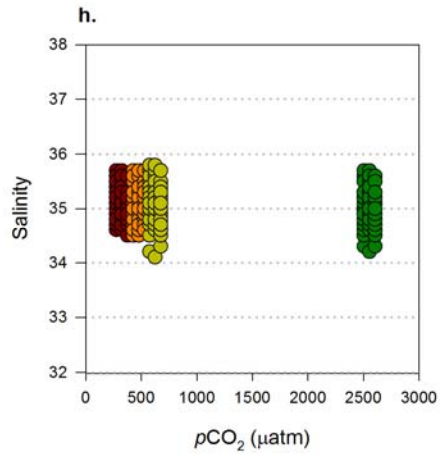
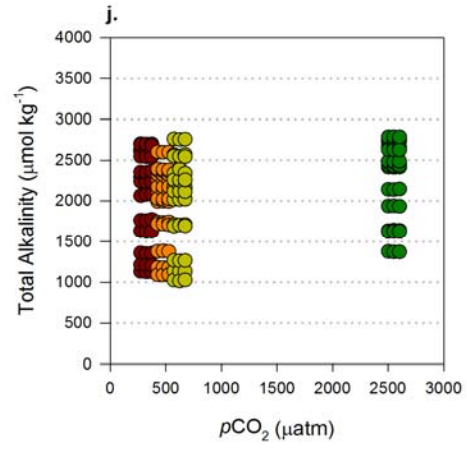
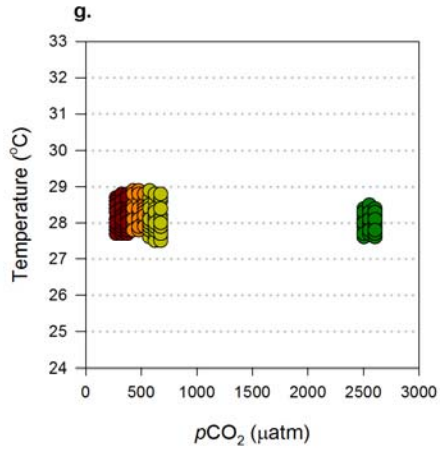
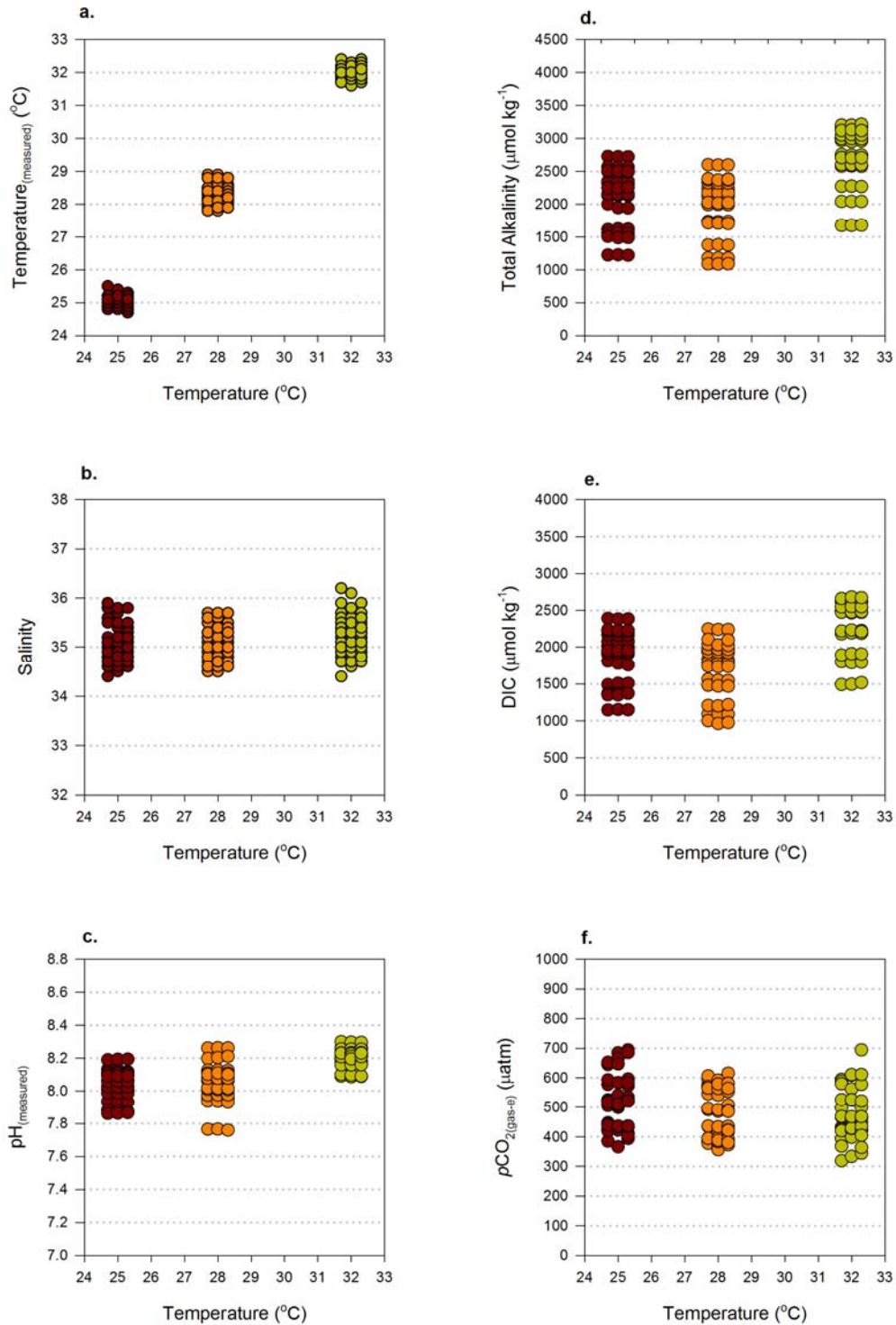


Figure S4. Measured and calculated parameters for temperature treatments over the 95-day experimental interval: measured temperature (a); measured salinity (b); measured pH (c); measured total alkalinity (d); measured dissolved inorganic carbon (e); calculated $p\text{CO}_2$ of the mixed gases in equilibrium with the experimental seawaters (f); calculated pH (g); calculated carbonate ion concentration (g); calculated bicarbonate ion concentration (i); calculated dissolved carbon dioxide (j); and calculated aragonite saturation state (k).



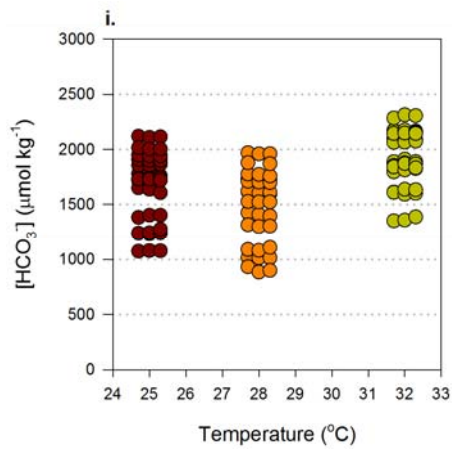
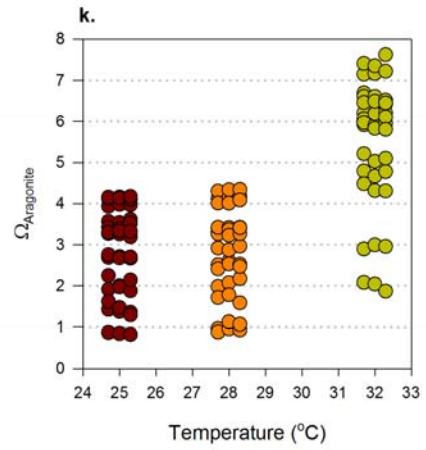
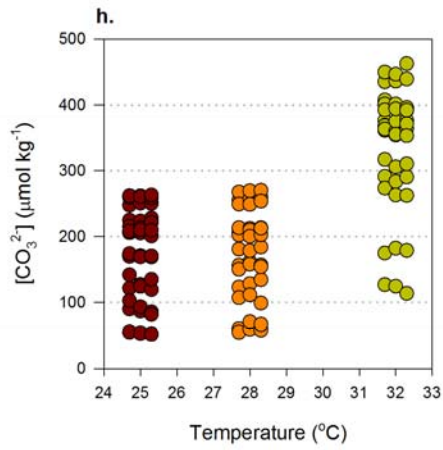
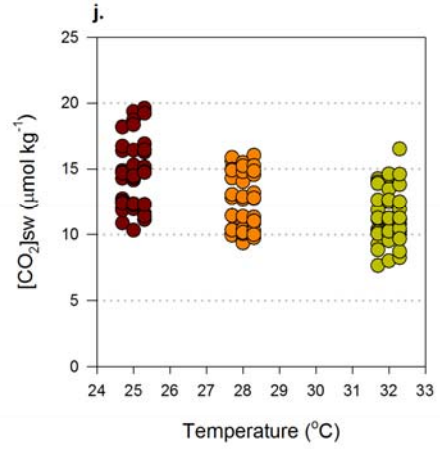
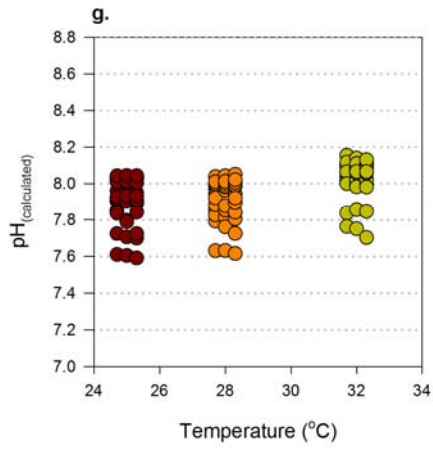


Figure S5. Final buoyant weight vs. final dry weight for 60 randomly selected *S. siderea* coral specimens that were reared in the various $p\text{CO}_2$ and temperature treatments. The ' $p\text{CO}_2 = 477/\text{Temp} = 28\text{ }^\circ\text{C}$ ' treatment was used in both the $p\text{CO}_2$ and temperature experiments.

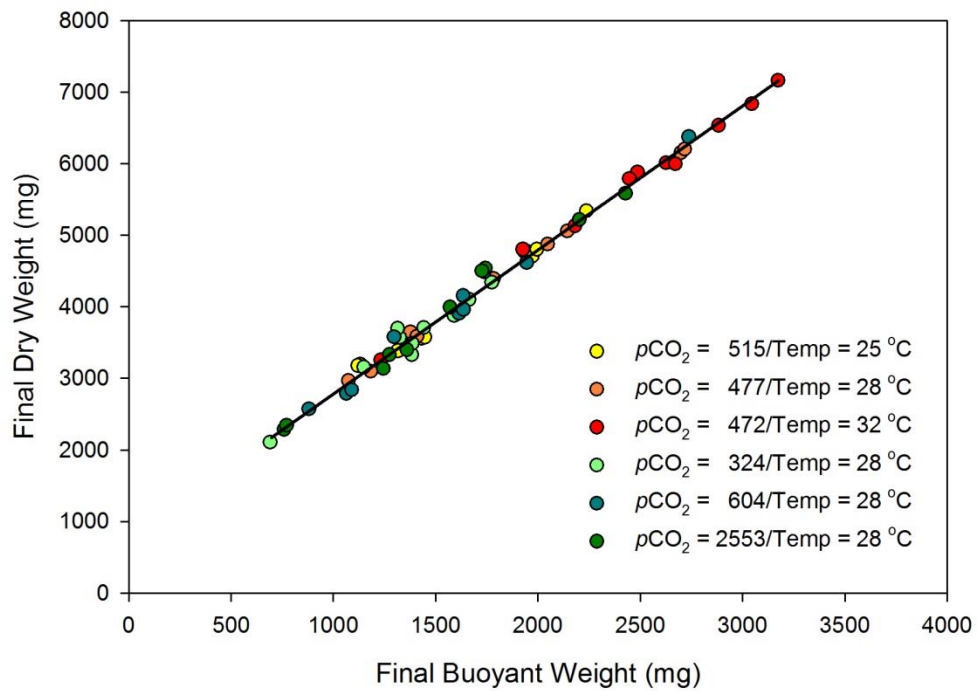


Figure S6. Relationship between maximum photosynthetic rate (ETR_{max}) and maximum photochemical efficiency of photosystem II (F_v/F_m) at dusk for several species of corals (data from Frade et al., 2008). Maximum photosynthetic rate (ETR_{max}) was estimated for corals in the present study (see Table S11; Figure 3) from average measured F_v/F_m using the approximately linear relationship (excluding the outlier) between Frade et al.'s (2008) F_v/F_m and ETR_{max} data (black line; $ETR_{max} = -186.08*(F_v/F_m) + 172.64$).

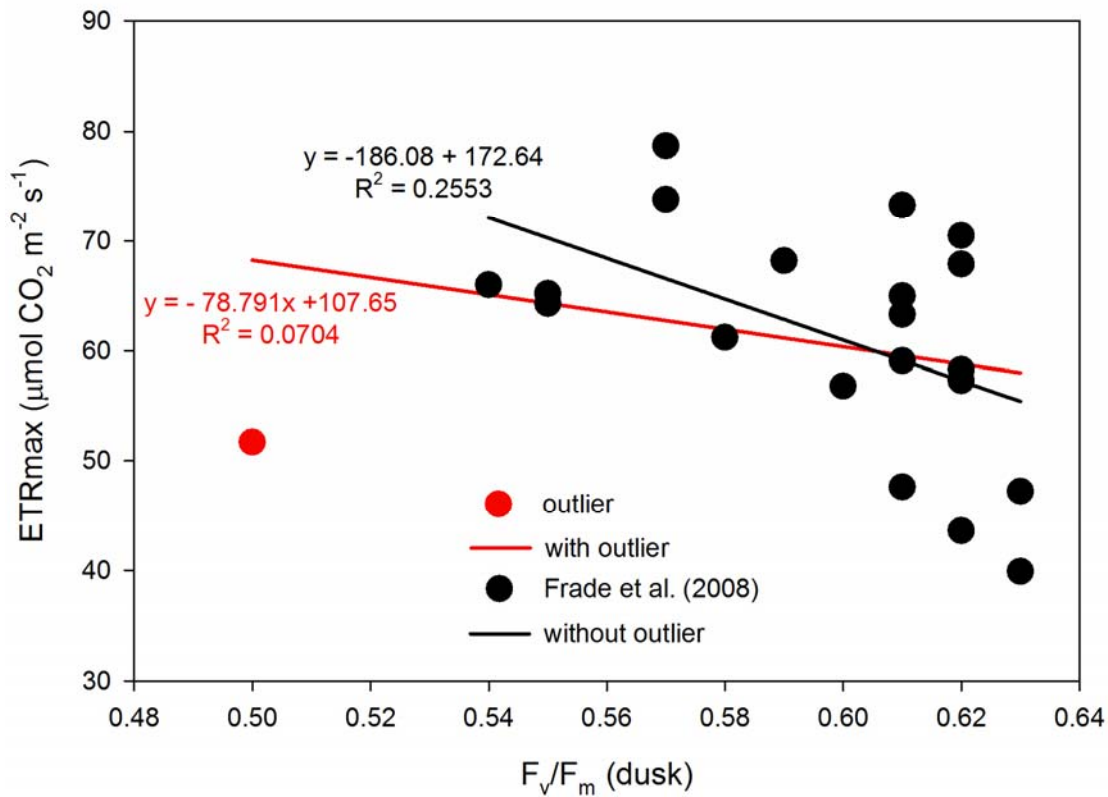


Figure S7. Average calcification rates for *S. siderea* coral specimens from the three reefzones (forereef, backreef, nearshore) reared at the four $p\text{CO}_2$ levels. The 95% confidence intervals (thin bars) and 73% confidence intervals (thick bars) can be used for making pairwise comparisons amongst corals from the different reefzones. Neither set of confidence intervals reveals a statistically significant difference in calcification rates amongst corals from the different reefzones reared within the same $p\text{CO}_2$ treatment.

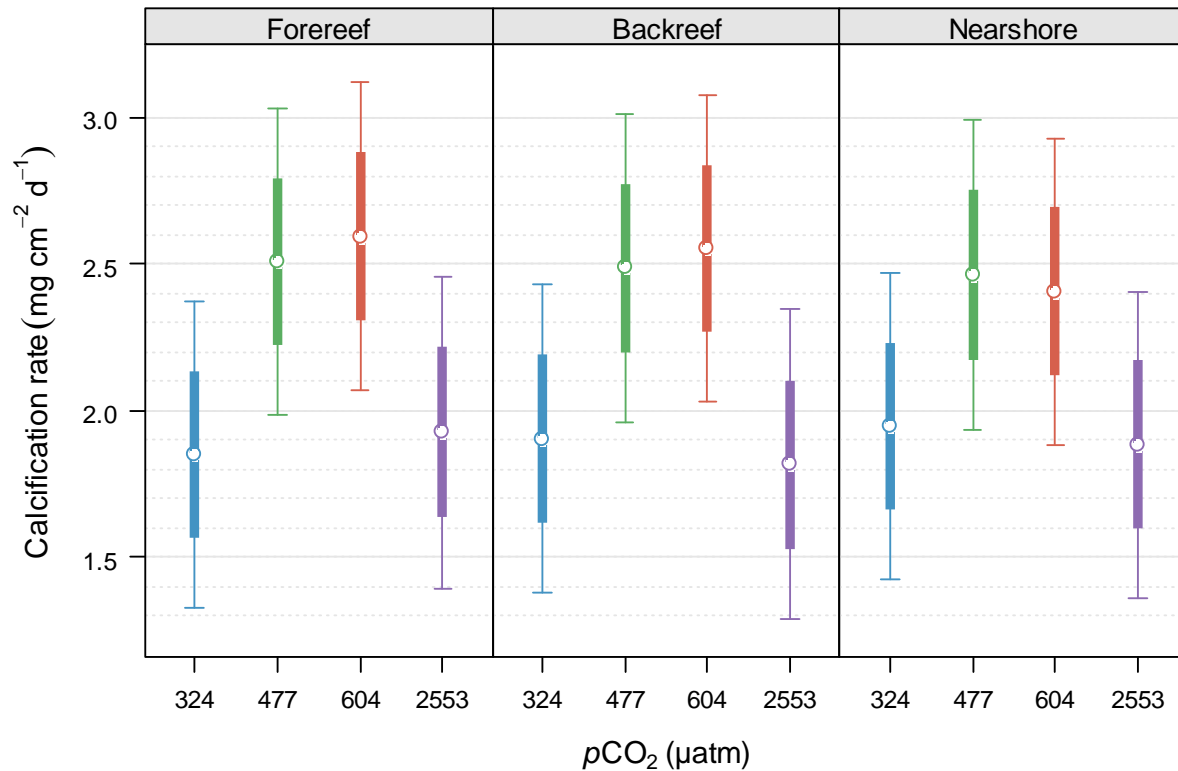
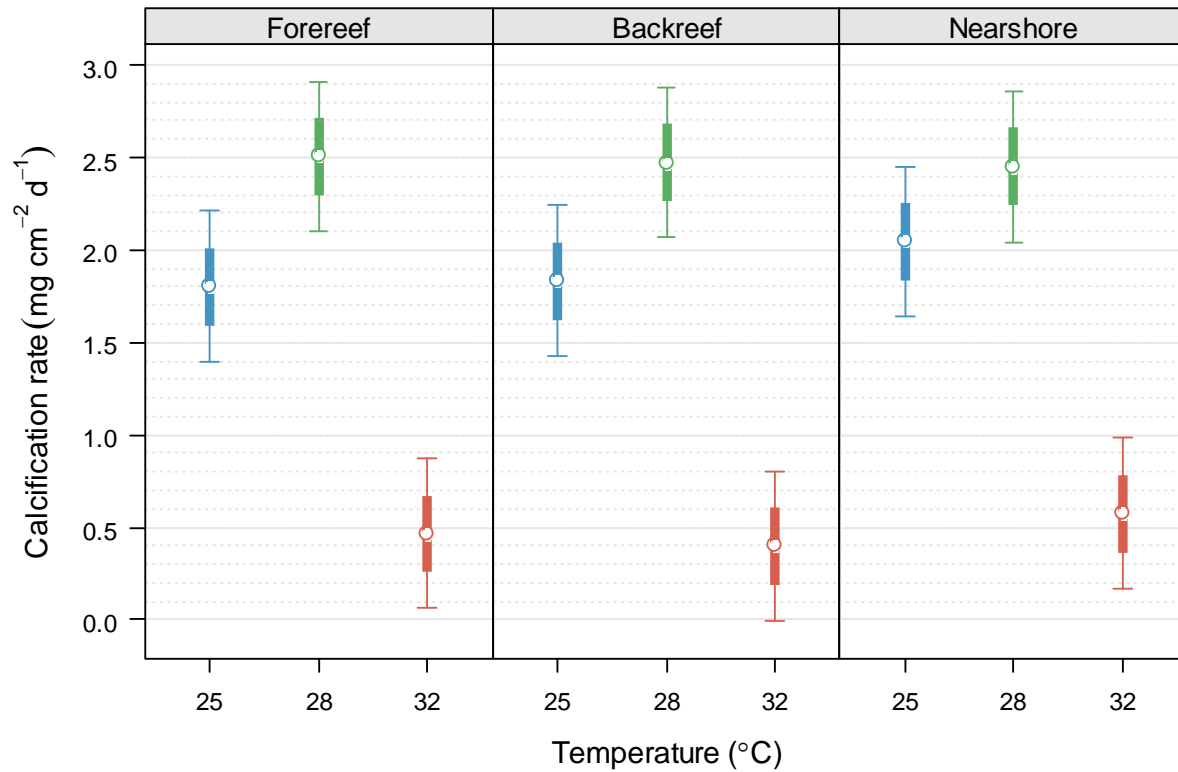


Figure S8. Average calcification rates for *S. siderea* coral specimens from the three reefzones (forereef, backreef, nearshore) reared at the three temperature levels. The 95% confidence intervals (thin bars) and 73% confidence intervals (thick bars) can be used for making pairwise comparisons amongst reefzones. Neither set of confidence intervals reveals a statistically significant difference in calcification rates amongst corals from the different reefzones reared within the same temperature treatment.



Supplementary References

- 1 Valiela, I. *Marine Ecological Processes*. (Springer, 1984).
- 2 Williams, G. J. *et al.* Ocean warming and acidification have complex interactive effects on the dynamics of a marine fungal disease. *Proceedings of the Royal Society B: Biological Sciences* 281, doi:10.1098/rspb.2013.3069 (2014).
- 3 Lewis, E. & Wallace, D. CO₂SYS: Program developed for CO₂ system calculations, ORNL/CDIAC-105. (1998).
- 4 Roy, R. *et al.* The dissociation constants of carbonic acid in seawater at salinities 5 to 45 and temperatures 0 to 45 °C. *Marine Chemistry* 44, 249-267, doi:10.1016/0304-4203(93)90207-5 (1993).
- 5 Mucci, A. The solubility of calcite and aragonite in seawater at various salinities, temperatures, and one atmosphere total pressure. *American Journal Science* 283, 780-799, doi:10.2475/ajs.283.7.780 (1983).
- 6 Hofmann, G. E. *et al.* High-Frequency Dynamics of Ocean pH: A Multi-Ecosystem Comparison. *PLoS ONE* 6, e28983, doi:10.1371/journal.pone.0028983 (2011).
- 7 Baguley, T. *Serious stats: A guide to advanced statistics for the behavioral sciences*. (Basingstoke: Palgrave, 2012).
- 8 Baguley, T. Calculating and graphing within-subject confidence intervals for ANOVA. *Behaviour Research Methods* 44, 158-175, doi:10.3758/s13428-011-0123-7 (2012).
- 9 SAS/STAT 13.1 User's Guide (SAS Institute Inc.), Cary, NC, 2013).
- 10 Plummer, M. in *Proceedings of the 3rd International Workshop on Distributed Statistical Computing*, . 20-22.
- 11 Frade, P., Bongaerts, P., Winkelhagen, A., Tonk, L. & Bak, R. In situ photobiology of corals over large depth ranges: A multivariate analysis on the roles of environment, host, and algal symbiont. *Limnology and Oceanography* 53, 2711-2723, doi:10.4319/lo.2008.53.6.2711 (2008).